State of Oregon
Oregon Department of Geology and Mineral Industries
Brad Avy, State Geologist

GEOLOGIC MAP 120

GEOLOGIC MAP OF THE DEVINE RIDGE SOUTH 7.5' QUADRANGLE, HARNEY COUNTY, OREGON

by Clark A. Niewendorp[1], Carlie J. M. Duda[2], Robert A. Houston[3], and Jason D. McClaughry[4]

2018

[1] Retired from Oregon Department of Geology and Mineral Industries, 800 NE Oregon Street, Suite 965, Portland, OR 97232
[2] Oregon Department of Geology and Mineral Industries, 800 NE Oregon Street, Suite 965, Portland, OR 97232
[3] Oregon Department of Geology and Mineral Industries, Springfield Field Office, Springfield Interagency Office, 3106 Pierce Pkwy D, Springfield, OR 97477
[4] Oregon Department of Geology and Mineral Industries, Baker City Field Office, Baker County Courthouse, 1995 3rd Street, Suite 130, Baker City, OR 97814

NOTICE

This manuscript is submitted for publication with the understanding that the United States Government is authorized to reproduce and distribute reprints for governmental use. The views and conclusions contained in this document are those of the authors and should not be interpreted as necessarily representing the official policies, either expressed or implied, of the U.S. government.

This product is for informational purposes and may not have been prepared for or be suitable for legal, engineering, or surveying purposes. Users of this information should review or consult the primary data and information sources to ascertain the usability of the information. This publication cannot substitute for site-specific investigations by qualified practitioners. Site-specific data may give results that differ from the results shown in the publication.

Cover photograph: A dome-like mass of dacite in the Devine Ridge South 7.5′ quadrangle, Harney County *(*43.745757, −118.945456 WGS84 geographic coordinates; 4845475mE, 343359mN WGS84 UTM Zone 11 coordinates). View looking north*.* Photo credit: Clark Niewendorp, August 2, 2017

Oregon Department of Geology and Mineral Industries Geologic Map Series GMS-120
Published in conformance with ORS 516.030.

For additional information:
Administrative Offices
800 NE Oregon Street, Suite 965
Portland, OR 97232
Telephone (971) 673-1555
Fax (971) 673-1562
https://www.oregongeology.org
https://www.oregon.gov/dogami

TABLE OF CONTENTS

LIST OF FIGURES

LIST OF TABLES

GEODATABASE

DRS2018_NCGMP09_v10.1.gdb

See the appendix for geodatabase description.

Geodatabase is Esri® version 10.1 format.

SHAPEFILES AND SPREADSHEETS

Shapefiles

Geochemistry: DRS2018_Geochemistry.shp
Bedding: DRS2018_Bedding.shp
Water Wells: DRS2018_WaterWells.shp
Springs: DRS2018_Springs.shp
Reference map: DRS2018_RefMap.shp
Cross Section Lines: DRS2018_XSectionLines.shp

Spreadsheets*

Geochemistry: DRS2018_Geochemistry.xlsx
Bedding: DRS2018_Bedding.xlsx
Water Well: DRS2018_WaterWells.xlsx
Springs: DRS2018_Springs.xlsx

*Master Excel file DRS2018_DATA contains the spreadsheets.

See the digital publication folder for files.
Metadata is embedded in the geodatabase and shapefiles and is also provided as separate .xml format files.

MAP PLATE

Plate 1. Geologic map of the Devine Ridge South 7.5′ quadrangle, Harney County, Oregon

See the digital publication folder for file.

1.0 INTRODUCTION

The Oregon Department of Geology and Mineral Industries (DOGAMI) mapped the geology of the Devine Ridge South 7.5-minute quadrangle, Harney County, Oregon, during 2017 and 2018. This mapping is part of a multi-year geologic study of the Harney Basin, designated a high priority by the Oregon Geologic Map Advisory Committee (**Figure 1-1**; **Figure 2-1**; Plate 1). Key objectives of this project include: (1) provide an updated and spatially accurate geologic framework for the Devine Ridge South 7.5′ quadrangle; (2) correlate lithologic units to surrounding areas; and (3) describe the occurrence of geologic resources (aggregate, industrial, mineral, and energy) and geologic hazards within the quadrangle. This study was supported in part by a grant from the STATEMAP component of the National Cooperative Geologic Mapping Program (G17AC00210). Additional funds were provided by the State of Oregon.

The core products of this study are this report, an accompanying geologic map and cross section, and an Esri ArcGIS® ArcMap™ geodatabase. The geodatabase presents new geologic mapping in a digital format, consistent with the U.S. Geological Survey (USGS) National Cooperative Geologic Mapping Program 2009 draft standard format for digital publication of geologic maps, version 1.1 (NCGMP, 2010). It contains spatial information about geologic polygons, contacts, and structures, and basic data (if available) about each geologic unit such as age, lithology, mineralogy, and structure. The geologic map and cross section, showing the distribution of bedrock lithology, critical structural relationships, and surficial geology, are at a scale of 1:24,000 (Plate 1).

Figure 1-1. Location map of the Devine Ridge South 7.5' quadrangle (this study) and the hydrologic boundary of the Harney Basin. Black rectangle outlines the study area. Base map: 10-m digital elevation model (DEM) shaded relief image.

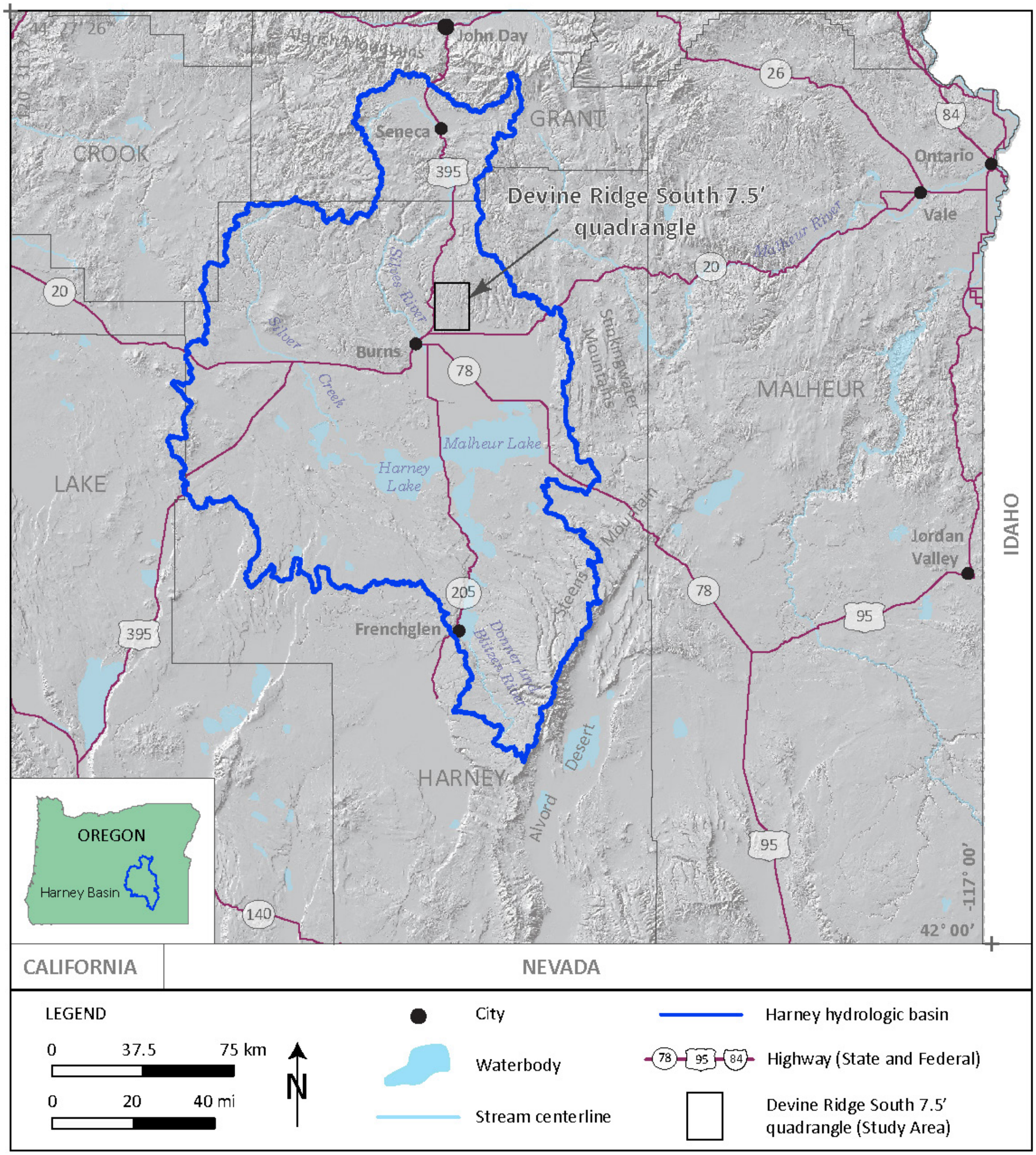

2.0 GEOGRAPHIC, ECOLOGIC, AND REGIONAL GEOLOGIC SETTINGS

The Harney hydraulic basin (HHB) encompasses an area of approximately 13,566 km^2 (5,238 mi^2) in southeastern Oregon (**Figure 1-1**). This basin is internally drained and fed by several creeks and rivers, including Silver Creek, Silvies River, and the Donner und Blitzen River (**Figure 1-1**). These tributaries drain into numerous plains, marshes, and lakes, including Harney Lake and Malheur Lake, which lie near the geographic center of the basin. Topographic relief is substantial, ranging from a high of 2,967 m (9,733 ft) at the summit of Steens Mountain to a low of 1,248 m (4,093 ft) at Harney Lake in the center of the basin. Climate in this region is semi-arid and precipitation amounts (rainfall and snow) vary greatly from year to year.

The HHB straddles the boundaries of three physiographic provinces in Oregon: Blue Mountains (BM), High Lava Plains (HLP), and Basin and Range (BR) (Walker and MacLeod, 1991; **Figure 2-1**). The northern third of the Harney Basin extends into the BM while the middle part of the basin bisects the HLP. The southern third of the basin encompasses the northern part of the BR.

The Blue Mountains are a geologic patchwork of four separate terranes: Baker, Wallowa, Olds Ferry, and Izee. Although not exposed in the map area, the pre-Cenozoic basement of the Izee Terrane is found in the northern Harney Basin less than 19 km (12 mi) to the north. The basement rocks are unconformably overlain by a diverse assemblage of middle Miocene and younger lavas, fluvial and lacustrine sedimentary rocks, and widespread ash-flow tuffs (**Figure 2-2**). Rocks in the central part of the basin are characterized by multiple episodes of late Miocene and younger bimodal volcanism (**Figure 2-1**, **Figure 2-2**) (MacLeod and others, 1976; Jordan and others, 2004). Also, central and marginal parts of the Harney Basin are covered by sequences of Quaternary sediments (<100 m thick) and several seasonal lakes. The BR is marked by large displacement (>150 m; >500 ft) north-northeast to northwest trending normal faults (e.g., Winter Rim Fault, Abert Rim Fault, Hart Mountain Fault, Steens Mountain Fault). BR deformation began during the Miocene (~17 Ma; Donath, 1962; Thompson and Burke, 1974).

The Brothers fault zone (BFZ) lies across the southern part of the basin as a wide, diffuse zone interpreted as an intracontinental transform fault separating the extended crust of the BR from comparatively un-extended BM crust to the north (Lawrence, 1976) (**Figure 2-1**, **Figure 2-2**). Lawrence (1976) described the BFZ as a series of longer (up to 20 km; 12.4 mi) discontinuous én echelon faults (Reidel shears) trending ~N50°W and less abundant shorter (5 km; 3.1 mi) N30°E faults expressed as horsts and grabens (Lawrence, 1976). Trench (2008) suggested east-west extension in the Basin and Range Province is accommodated by dextral oblique strike-slip horsetail fractures in the BFZ that resulted from structural clockwise rotation about a pole located in northeastern Oregon.

The study area is in the northern portion of the HHB and the rocks there can be divided into three distinct assemblages:

- The 15.6 to 16.5 Ma Steens Basalt, the earliest lavas to erupt as part of the Columbia River Basalt Group (CRBG), are exposed in the southern part of the HHB (**Figure 2-2**) and cover much of southeastern Oregon and parts of southwestern Idaho to northern Nevada (Scarberry and others, 2007). The 16.1 Ma Picture Gorge Basalt (Baksi, 1989) of the CRBG largely occurs in north-central Oregon and extends south to the northern part of the Harney Basin (Cahoon and Streck, 2017).
- Three late Miocene ash-flow tuffs (Harney Basin Volcanic Field) and one middle Miocene ash-flow tuff (Lake Owyhee Volcanic Field) are important stratigraphic markers in the map area. These ash-flow tuffs overlie older CRBG units and include the ~16 Ma Dinner Creek Tuff (**Tmdc**), 9.63 Ma Devine Canyon Ash-flow Tuff (**Tmtd**) (Ford and others, 2013), 8.41 Ma Prater

Creek Ash-flow Tuff (**Tmtp**) (Jordan and others, 2004), and 7.05 Ma Rattlesnake Tuff (**Tmtr**) (Streck and Grunder, 1995). The areal extents of some of these ash-flow tuffs are up to tens of thousands square kilometers. From the thickness and distribution of the Rattlesnake Tuff and Prater Ash-flow Tuff, the inferred caldera sources for these tuffs is buried and may be from areas somewhere in the HHB's lowland to the south and southwest of the study area (Greene, 1972; Streck, 1994). The caldera source for the Devine Canyon Ash-flow Tuff could be elsewhere according to J. D. McClaughry (2018, verbal commun.), although Greene (1973) and Khatiwada and Keller (2015) suggested the distribution of this tuff indicates a source area that is also buried below the lowland.

- According to M. L. Ferns (2018, written commun.), mafic suites overlying the Rattlesnake Tuff appear to be alkali intermediate rocks that are likely associated with the Rattlesnake Tuff and Prater Creek Ash-flow Tuff vents. Most if not all the true olivine basalts of the High Lava Plains are younger and are associated with vents along the Brothers Fault Zone (Reidel and others, 2002).

Figure 2-1. Physiographic province map of Oregon, showing location of the Brothers Fault Zone and the study area. Solid grey lines demarcate physiographic provinces (after Orr and others, 1992; Walker, 1977). Blue line marks the location of the Harney hydrologic basin. Box denotes the study location. Base map: 10-m digital elevation model (DEM) shaded relief image. The length and width of the Brothers Fault Zone is generalized.

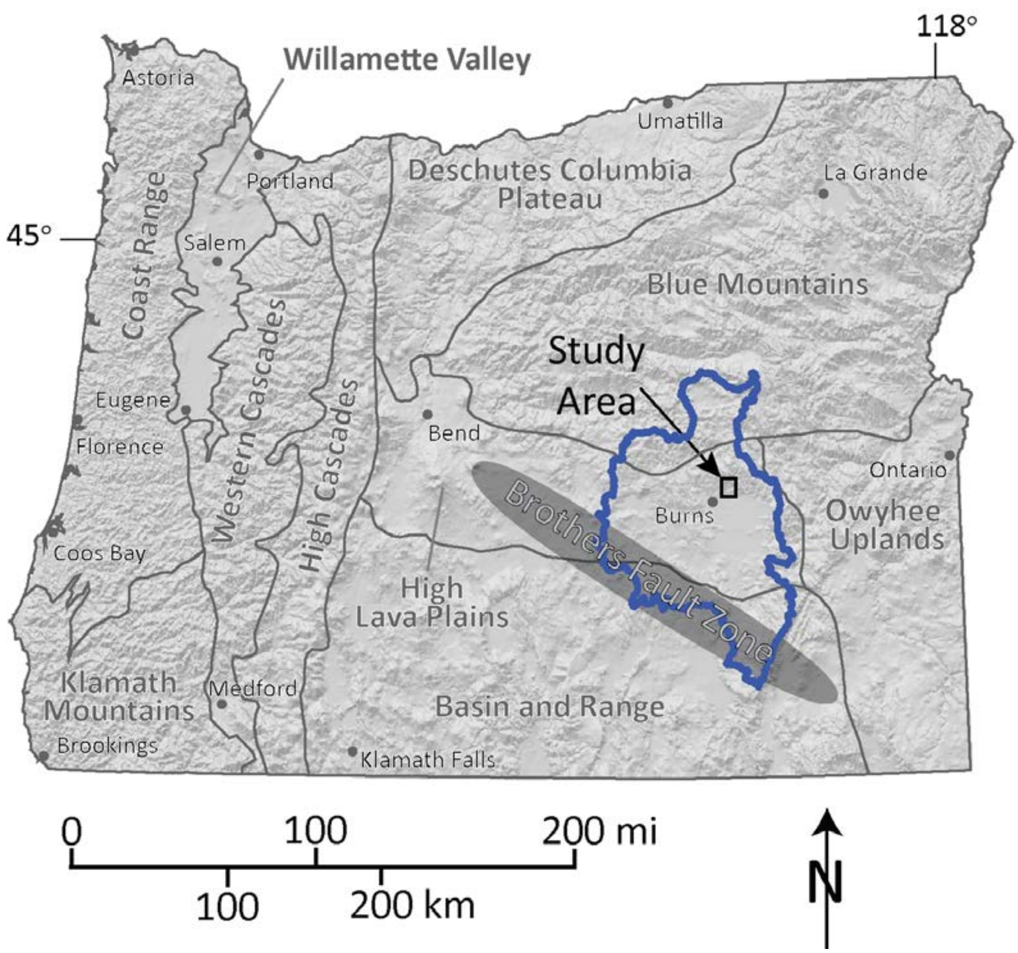

Figure 2-2. Generalized geologic map of southeastern Oregon (after Smith and Roe, 2015). Red box denotes study location.

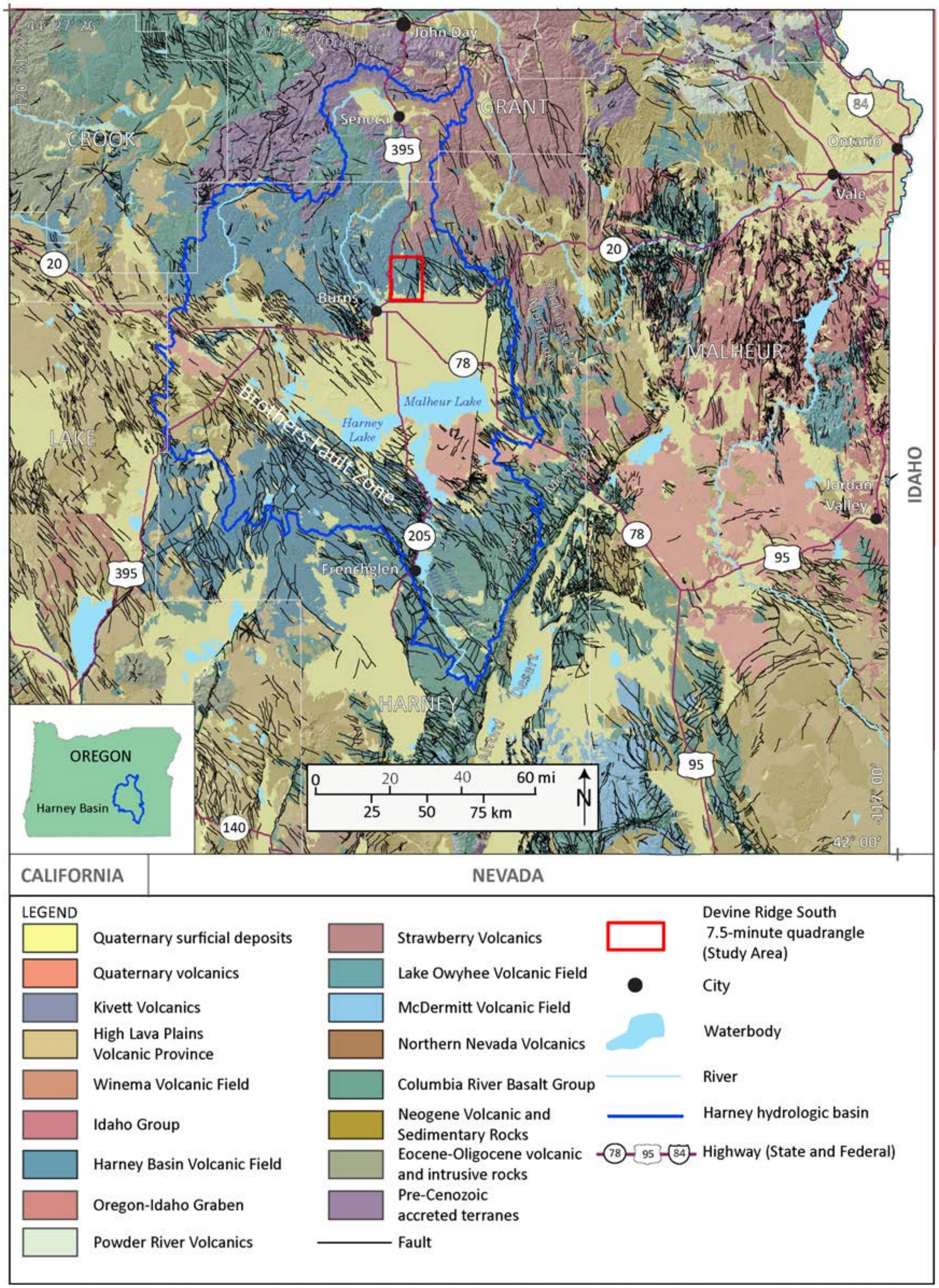

3.0 PREVIOUS WORK

The study builds on previous regional geologic mapping, groundwater studies, and natural resource investigations by Russell (1884), Piper and others (1939), Wallace and Calkins (1956), Walker and Repenning (1965), Brown and Thayer (1966), Greene (1972), Greene and others (1972), Greene (1973), Niem (1974), Lawrence (1976), Walker (1979), Brown and others (1980), Brown (1982), Gray and others (1983), McGrane (1985), Minor and others (1987a,b), Johnson (1994), Sheppard and Gude (1993), Sherrod and Johnson (1994), Streck and Grunder (1995), Johnson (1996, 1998), Camp and others (2003), Streck and Ferns (2004), Scarberry and others (2007), Trench (2008), Meigs and others (2009), Milliard (2010), Boschmann (2012), Ferns and McClaughry (2013), Ford and others (2013), Camp and others (2013), Khatiwada and Keller (2015), and Streck and others (2015). This study also used unpublished data (N. S. Wagner, unpub. data, 1944; S. L. Isom and M. J. Streck, unpub. data, 2017; R. A. Houston and others, unpub. data, 2016; R. A. Houston and others, unpub. data, 2017; M. Cruz and M. J. Streck, unpub. data, 2017). The index map shown in **Figure 3-1** summarizes the sources of regional geologic maps used during the preparation of the Devine Ridge South 7.5′ quadrangle geologic map (Plate 1).

Figure 3-1. Sources of regional geologic mapping used during the preparation of this report. In the geodatabase, see DataSourcePolys feature class. Red box denotes study location. Base map: 10-m digital elevation model (DEM) shaded relief image.

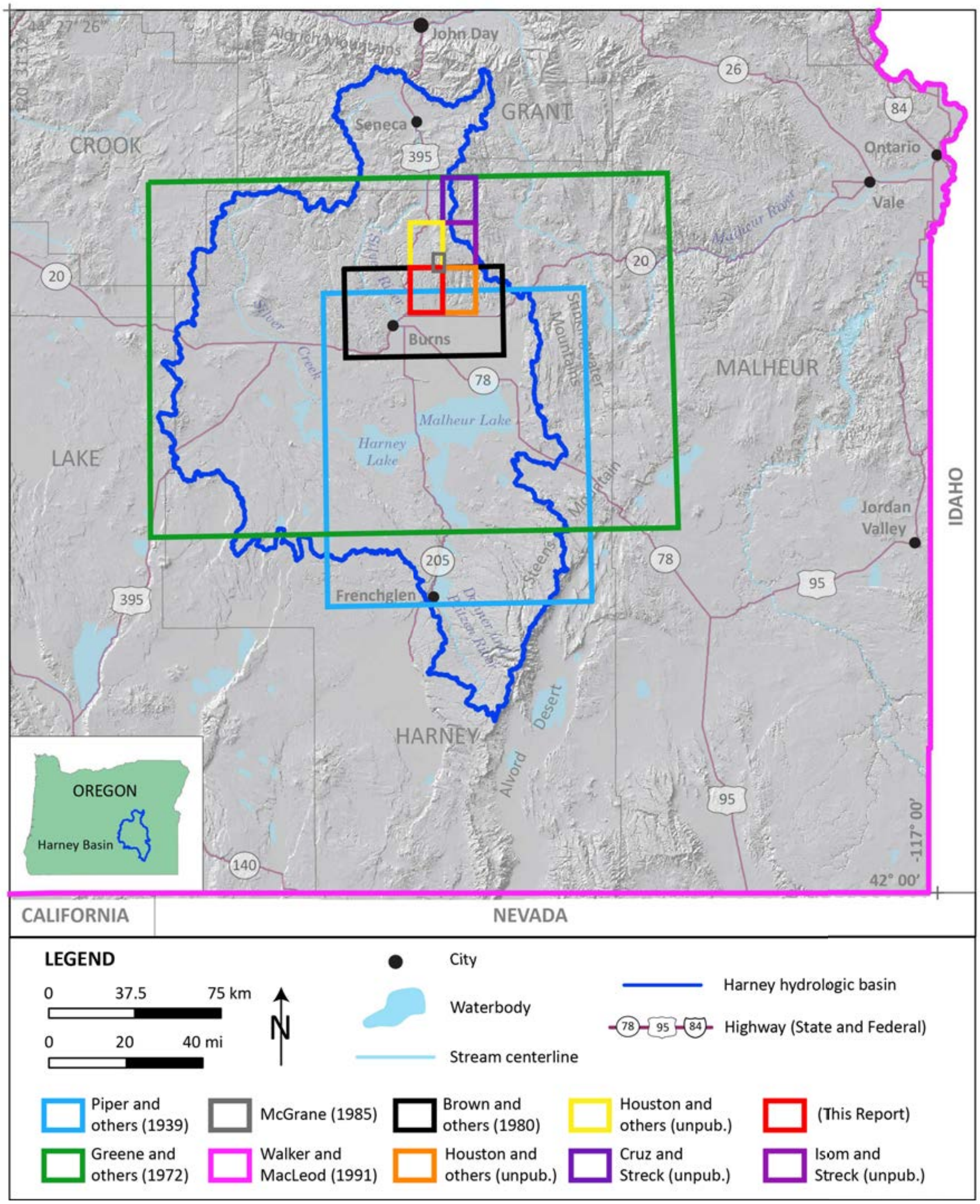

4.0 METHODOLOGY

Geologic data were collected digitally using a GPS-enabled Apple® iPad® 4 and an GPS-enabled Apple iPhone® 7, both loaded with Geometry Pty Ltd iGIS Pro, a geographic information system software package compatible with Esri ArcGIS. Geologic mapping used a 5-m Structure from Motion (SFM) digital elevation model (DEM) derived hillshaded image, USGS digital raster graphics (DRGs), and digital orthophoto imagery (2016) obtained from Google Earth™ as basemaps. Fieldwork conducted during this study consisted of data collection along roads, combined with transects following lithologic contacts and faults across public and private timber and rangelands. Standard geologic methods for collecting samples and measuring attitudes of inclined bedding, geologic features, and faults were employed. Digitization and the final digital Esri ArcGIS ArcMAP format geologic database were completed at a minimum scale of 1:24,000.

Mapping was supported by new and compiled X-ray fluorescence (XRF) geochemical analyses of whole-rock samples, thin-section petrography, and field and remotely collected strike and dip measurements of inclined bedding (Plate 1). Whole-rock geochemical samples were prepared and analyzed by XRF at the Washington State University GeoAnalytical Lab, Pullman, Washington, under the direction of Dr. Scott Buroughs. Analytical procedures for the Washington State University GeoAnalytical Lab are described by Johnson and others (1999) and can be obtained online at https://s3.wp.wsu.edu/uploads/sites/2191/2017/06/Johnson-Hooper-and-Conrey.pdf. Major element determinations were normalized to a 100-percent total on a volatile-free basis and recalculated with total iron expressed as FeO*. Whole-rock geochemical data are useful in classifying volcanic rocks, as many lavas are too fine grained and glassy to be adequately characterized by mineralogical criteria alone. Descriptive rock unit names for volcanic rocks are based in part on the online British Geological Survey classification schemes (Gillespie and Styles, 1999; Robertson, 1999; Hallsworth and Knox, 1999) and normalized major element analyses plotted on the total alkali ($Na_2O + K_2O$) versus silica (SiO_2) diagram (TAS) of Le Bas and others (1986), Le Bas and Streckeisen (1991), and Le Maitre and others (1989, 2004).

Microsoft Excel® spreadsheets tabulating geochemical analyses, water wells, and strike and dip measurements are provided as part of this publication and accompany the geodatabase (see page 6 of this report). The **APPENDIX** contains a summary of data collection methods and the field list for the spreadsheets mentioned above.

In this report, volcanic rocks with fine-grained (<1 mm [0.04 in]; Mackenzie and others, 1997; Le Maitre and others, 2004), average crystal or particle size in the groundmass are characterized in the following manner:

- A “coarse groundmass” if the average crystal or particle size is <1 mm (0.04 in) and can be determined using the naked eye (>~0.5 mm [0.02 in]).
- A “medium groundmass” if crystals of average size cannot be determined by eye but can be distinguished by using a hand lens (>~0.05 mm [0.02 in]).
- A “fine groundmass” if crystals or grains of average size can be determined only by using a microscope (or by hand lens recognition of phyllite-like sparkle or sheen in reflected light, indicating the presence of crystalline groundmass).
- A “glassy groundmass” if the groundmass has (fresh), or originally had (altered), groundmass with the characteristics of glass (conchoidal fracture; sharp, transparent edges; vitreous luster; etc.).

- Mixtures of crystalline and glassy groundmass are described as intersertal; ratios of glass to crystalline materials may be indicated by textural terms including holocrystalline, hypocrystalline, hyalophitic, and hyalopilitic.
- Microphenocrysts are defined as crystals larger than the overall groundmass and < 1 mm across (0.04 in).

Grain size of clastic sedimentary rocks is described following the Wentworth (1922) scale. Hand samples of unconsolidated sediments and clastic sedimentary rocks were compared in the field and/or in the laboratory to graphical representations (comparator) of the Wentworth scale to determine average representative grain size in various parts of a respective sedimentary geologic unit. Colors given for hand-sample descriptions are from the Geological Society of America Rock-Color Chart Committee (1991).

Subsurface geology shown in the geologic cross section (Plate 1) incorporates lithologic interpretations from water-well drill records available through the Oregon Water Resources Department (OWRD) Groundwater Resource Information Distribution (GRID)system (**APPENDIX**). Water wells were not physically located. However, an attempt was made remotely to locate water wells and other drill holes that have well logs archived by OWRD. Approximate locations were estimated by using a combination of sources, including internal OWRD databases of located wells, Google Earth™, tax lot maps, street addresses, and aerial photographs. The accuracy of the locations ranges widely, from errors of 1.1 km (0.7 mi) possible for wells located only by section and plotted at the section centroid to a few tens of feet for wells located by address or tax lot number on a city lot with bearing and distance from a corner. A well log ID is queried in the database (e.g., HARN-51852) to retrieve an image of the well log from the OWRD web site (https://apps.wrd.state.or.us/apps/gw/well_log/). A database of well logs with interpreted subsurface geologic units for the Devine Ridge South 7.5′ quadrangle is provided with the geodatabase.

To allow the interested reader to visit these sites in the field or to visualize remotely the area by using Google Earth™, map coordinates are provided for outcrop photographs shown in report figures. Locations are provided in two coordinate systems: (1) Geographic (datum = WGS84, units = decimal degree); and (2) Universal Transverse Mercator (UTM) Zone 11 (datum = WGS84, units = meters). Decimal degree coordinates can be entered into the “Fly to” box (e.g., 45.661323, -121.471230) in the search toolbar, and Google Earth™ will automatically locate and “fly” to the specified site.

5.0 EXPLANATION OF MAP UNITS

The stratigraphic positions of terrestrial sedimentary and volcanic bedrock units in the Devine Ridge South 7.5′ quadrangle range from upper Oligocene to upper Miocene (**Figure 5-1**; Plate 1). Bedrock geologic units are locally covered along drainages and on some slopes in the project area by Pleistocene and Holocene surficial deposits. Widely separated stratigraphic units were grouped because of apparent stratigraphic position, lithology, and chemical composition. Unit names follow local stratigraphic nomenclature when available, but when formal rock names are lacking, informal names are given because of composition or sites of good exposure. **Figure 5-1** depicts a time-rock chart showing age ranges for Cenozoic bedrock and surficial units.

5.1 Overview of map units

UPPER CENOZOIC SURFICIAL DEPOSITS

Qf modern fill and construction material (upper Holocene)
Qa alluvium (Holocene and Upper Pleistocene[?])
Qaf fan deposits (Holocene and Upper Pleistocene[?])
Qls landslide deposits (Holocene and Upper Pleistocene[?])
Qao older alluvium (Holocene and Upper Pleistocene[?])
Qlo loess (Holocene[?] and lower Pleistocene[?])

Angular unconformity to disconformity

UPPER TO LOWER CENOZOIC VOLCANIC AND SEDIMENTARY ROCKS

LOWER PLEISTOCENE TO UPPER MIOCENE SEDIMENTARY ROCKS

QTst sedimentary rocks (lower Pleistocene[?] and upper Miocene[?])

UPPER TO MIDDLE MIOCENE VOLCANIC AND SEDIMENTARY ROCKS

Tmtr Rattlesnake Tuff (upper Miocene) 7.05 ± 0.01 Ma ($^{40}Ar/^{39}Ar$); 7.093 ± 0.015 Ma ($^{40}Ar/^{39}Ar$)
Tmtp Prater Creek Ash-flow Tuff (upper Miocene) 8.41 ± 0.16 Ma ($^{40}Ar/^{39}Ar$)
Tmtd Devine Canyon Ash-flow Tuff (upper Miocene) 9.63 ± 0.05 Ma ($^{40}Ar/^{39}Ar$)
Tmst tuffaceous sedimentary rocks (upper Miocene[?] and middle Miocene[?])

Nonconformity

MIDDLE TO LOWER MIOCENE VOLCANIC ROCKS

Tmdc Dinner Creek Tuff (middle or lower Miocene) 15.9 ± 0.09 Ma ($^{40}Ar/^{39}Ar$); 16.16 ± 0.02 Ma ($^{40}Ar/^{39}Ar$)
Tmb basalt–basaltic andesite (lower Miocene[?])

Angular unconformity to disconformity

UPPER OLIGOCENE VOLCANIC ROCKS

Toa andesite (upper Oligocene) 24.75 ± 0.15 Ma ($^{40}Ar/^{39}Ar$)
Tor rhyolite (upper Oligocene[?])
Toda dacite (upper Oligocene[?])

Figure 5-1. Time-Rock chart of the Devine Ridge South 7.5' quadrangle showing the 16 geologic units shown on the geologic map and in the geologic cross section.

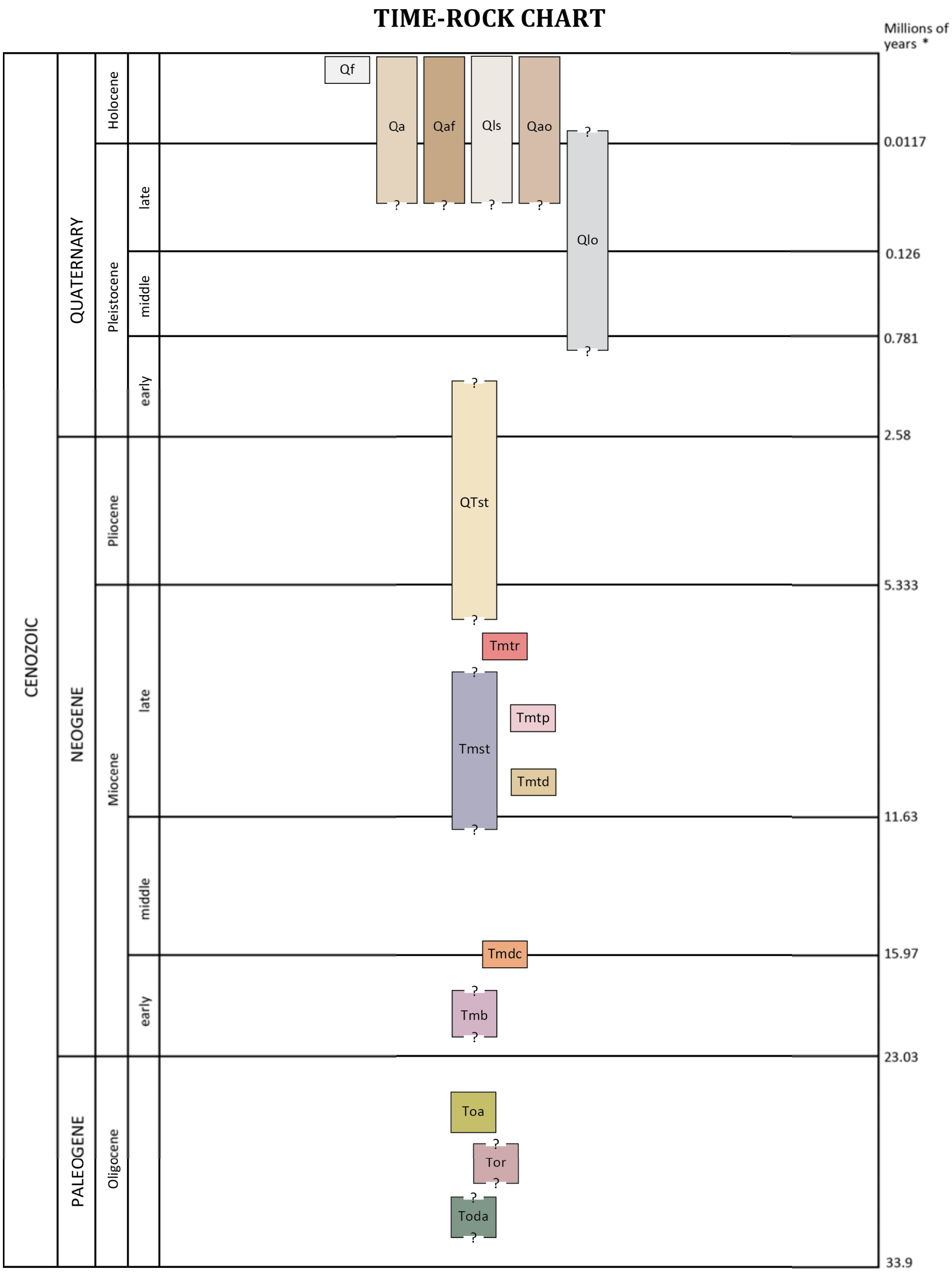

*International Chronostratigraphic Chart, International Stratigraphic Commission, 2013/V1, Time scale after Gradstein and others (2004), Ogg and others (2008), and Cohen and others (2013). http://www.stratigraphy.org/index.php/ics-chart-timescale

5.2 Upper Cenozoic surficial deposits

Late Cenozoic sedimentary and volcanic rocks exposed in the Devine Ridge South 7.5′ quadrangle are locally covered by Pleistocene and Holocene surficial deposits (**Figure 5-1**; Plate 1). Important surficial units include alluvial, landslide, and fan deposits. Surficial units within the project area are delineated on the basis of geomorphology as interpreted from a combination of field observations, 5-m SFM hillshaded DEM, and 2016 National Agriculture Imagery Program (NAIP) orthophotos.

Qf **modern fill and construction material (upper Holocene)**—Man-made deposits of poorly sorted and crudely layered mixed gravel, sand, clay, and other engineered fill (Plate 1). These deposits usually contain rounded to angular clasts ranging from small pebbles to boulders up to several meters across. The orientation of clasts is typically less uniform than is found in naturally occurring imbricated or bedding-parallel gravel. Deposits mapped as modern fill and construction material in the map area are generally associated with dams, road embankments, culvert fills, and mined land (**Plate 1**). The thickness of fill-deposits may exceed 30 m (98 ft).

Qa **alluvium (Holocene and Upper Pleistocene[?])**—Unconsolidated gravel, sand, silt, and clay deposited along active stream channels and on adjacent floodplains (**Figure 5-2**; Plate 1). Gravel deposited as imbricated, massive to cross-stratified accumulations on smaller mid-channel islands and bars is the most common type of near channel alluvium along major tributaries, such as Coffee Pot, Rattlesnake, and Cow Creeks. Thickness of alluvial deposits is generally less than 5 m (16 ft); bedrock units may be locally exposed in the base of stream channels within areas mapped as **Qa**. They may include deposits containing man-made debris or artifacts, or deposits filling areas known to have been modified by man such as railroad grades, excavations, roadways, or gravel pits. The unit is assigned a Holocene to late Pleistocene age on the basis of stratigraphic position.

Qaf **fan deposits (Holocene and Upper Pleistocene[?])**—Unconsolidated deposits of boulders, cobbles, pebbles, granules, sand, silt, clay, and woody debris preserved in fan-shaped accumulations at the transition between low-gradient valley floodplains and steeper upland drainages (Plate 1). Surfaces of fans are characterized by anastomosing, intermittent fluvial channels formed where pools or obstructions, such as log-jams or debris flow levees, create flow diversions. Sediment accumulates on the fan surface through normal fluvial deposition, avulsions, and lateral migration as streams emerge from upland settings and the gradient falls below the threshold for further sediment transport. Fans also accumulate during episodic high-discharge events as accumulations of soil, colluvium, large woody debris, or landslide deposits are remobilized and transported down slope as fast-moving sediment gravity flows (hyperconcentrated flood flows and debris flows). The unit may locally include rapidly deposited talus from rockfall in steep drainages. Fans typically have a steep gradient at the apex, moderate gradient through the middle section, and low gradient near the toe. Individual fans generally cover less than 1 hectare (2.5 acres). The local thickness of alluvial fan deposits is variable but is probably <15 m (50 ft). The unit is assigned a Holocene to late Pleistocene age on the basis of stratigraphic position.

Qls **landslide deposits (Holocene and Upper Pleistocene[?])**—Unconsolidated, chaotically mixed masses of rock and soil deposited by landslides (e.g., slumps, slides, debris flows, rock avalanches;

Plate 1). Deposits may consist of individual slide masses or may form large complexes resulting from multiple generations of landslide activity. Recent landslide terrain is characterized by sloping hummocky surfaces, locally marked by closed depressions, springs and wet seeps, and scarps. Active or recently active landslides are marked by marginal levees and open ground fissures; tilted trees and bent trunks may be common on the surface. Toes to more recent deposits retain convex-up, fan-shaped morphologies. Slides are often traceable uphill to headwall scarps or slip surfaces. In more deeply seated landslides, these head scarps commonly expose bedrock. The unit locally includes rock fall, large talus piles, shallow-seated landslides of colluvium, rapidly emplaced debris flow deposits, and more deeply seated bedrock slides. Quaternary landslide complexes in the map area are commonly small in extent, covering 1 hectare (2.5 acres) to 77 hectares (31 acres). Thickness of landslide deposits is highly varied but may be more than several tens of meters in larger deposits. Large areas mapped as unit **Qls** typically include many discrete deposits of varying ages that are not differentiated here. The unit is assigned a Holocene to late Pleistocene age on the basis of stratigraphic position.

Qao **older alluvium (Holocene and Upper Pleistocene[?])**—Moderately dissected, unconsolidated, well to poorly sorted and stratified gravel, sand, silt, and clay deposited in active stream channels and on adjoining flood plains (Plate 1). These deposits are recognized and mapped in the lower half of the quadrangle along Poison, Prater, and Soldier Creeks, where deposits reside adjacent to incised drainages filled with younger Quaternary alluvium (**Qa**). Thickness of the unit probably does not exceed 6 m (20 ft). The unit is assigned a Holocene to late Pleistocene age on the basis of stratigraphic position and a lack of more precise age indications.

Qlo **loess (Holocene[?] and lower Pleistocene[?])**—Very fine grained sand and clay mantles upland surfaces locally across the southeastern part of the quadrangle (Plate 1). Mazama ash, an airfall tuff, may be part of the unit. Thickness of the unit ranges from thin veneers < 1 m (3.3 ft) to as much as ~6 m (20 ft). The unit typically forms a massive featureless morphology. The distribution of loess is identified from field observations, 5-m SFM hillshaded DEMs, and 2016 NAIP orthophotos (Plate 1). Thinner or geographically restricted deposits have not been mapped where the underlying geology can be reasonably inferred or is known to be present at or near the surface. The unit is assigned a Holocene (?) to early Pleistocene (?) age on the basis of stratigraphic position.

Angular unconformity to disconformity

5.3 Upper to lower Cenozoic volcanic and sedimentary rocks

5.3.1 Lower Pleistocene to upper Miocene sedimentary rocks

QTst **sedimentary rocks (lower Pleistocene[?] and upper Miocene[?])**—White to buff, semi-consolidated to locally poorly indurated conglomerate and tuffaceous sandstone and mudstone are erosional remnants locally exposed in the southern portion of the study area. **QTst** crops out as rounded hills and overlies the Rattlesnake Tuff (**Tmtr**) (Plate 1). Total thickness in mapped area is probably < 27 m (90 ft).

According to Brown and others (1980), rocks equivalent to **QTst** are present in the Harney Formation type section at Wrights Point (Walker, 1977, 1979), about 18 km (11.5 mi) to the southeast of the study area. Other workers who have examined the Harney Formation include Piper and others (1939), Greene (1972), Greene and others (1972), and Niem (1974). The unit is assigned an early Pleistocene(?) to late Miocene(?) age on the basis of stratigraphic position.

5.3.2 Middle to upper Miocene volcanic and sedimentary rocks

Tmtr **Rattlesnake Tuff (upper Miocene)**—Vitric, crystal poor, pumice and lithic rich tuff, primarily exposed in the southern half of the map area. **Tmtr** is 10 to 22 m (32 to 72 ft) thick in the map area and represents a single cooling unit. A typical exposure of **Tmtr** in the map area is the lithophysal part of the unit. This zone forms distinctive outcrop cliffs and rimrock that can be easily traced throughout the map area. It is not uncommon to find float of the densely welded vitrophyre section of the Rattlesnake Tuff (**Tmtr**) at the bases of cliffs and rimrock and on top of low hills in the northwestern part of the map. The type section of the Rattlesnake Tuff (**Tmtr**) is exposed along U.S. Highway 395 in the southwest corner of the map area (Streck and Grunder, 1995) (**Figure 5-2**; Plate 1).

Typical hand samples are very pale orange (10YR 8/2), to very light gray (N7), to medium gray (N5), and light brownish gray (5YR 6/1), containing < 3 percent quartz, subhedral to euhedral, zoned anorthoclase and anhedral to euhedral clinopyroxene (ferrohedenbergite) micro-phenocrysts and phenocrysts <2 mm (0.01 in) distributed within a vitric groundmass. The tuff is petrographically characterized by ~2 percent quartz and feldspar phenocrysts, ~1 percent ferrohedenbergite phenocrysts, ~15 percent lithic fragments, ~15 percent pumice, and 55 percent devitrified glass-shard groundmass. The original vitroclastic texture of the tuff is retained but is locally overprinted by very fine elongated crystals forming axiolitic structures.

Samples obtained from the Rattlesnake Tuff have rhyolitic compositions ranging from 76.01 to 79.69 weight percent SiO_2, 10.63 to 12.72 weight percent Al_2O_3, 3.13 to 4.40 weight percent Na_2O, and 4.12 to 5.57 weight percent K_2O (R. A. Houston and others, unpub. data, 2016; R. A. Houston and others, unpub. data, 2017; Streck, 1994; and Streck and Grunder, 1995) (**Table 5-1**). The tuff also contains relatively moderate amounts of barium (364 to 808 ppm Ba), zirconium (260 to 312 ppm Zr), yttrium (82 to 115 ppm Y), and niobium (26 to 31 ppm Nb).

The unit is equivalent to the Rattlesnake Ash-flow Tuff as defined by Walker (1979) and the Rattlesnake Tuff (**Tmtr**) as renamed by Streck and Grunder (1995). Regionally, the Rattlesnake Tuff occurs as a thick blanket that covered at least 35,000 km^2 (13,500 mi^2) (Streck and Grunder, 1995). Streck (1994) proposed a vent located in the western Harney Basin, near Capehart Lake. The Rattlesnake Tuff has a reversed magnetic polarity (Parker, 1974; Thormahlen, 1984; Smith, 1986a,b; Streck, 1994) and is assigned a late Miocene age on the basis of stratigraphic position and $^{40}Ar/^{39}Ar$ ages of 7.05 ± 0.1 Ma (Streck, 1994) and 7.093 ± 0.015 Ma (Jordan and others, 2002).

Figure 5-2. Type locality of the Rattlesnake Tuff (Tmtr) about 16 km (10 mi) north of Burns along the west side of U.S. Highway 395. An outcrop photograph and a line drawing of zonal variations in the exposure of Rattlesnake Tuff are shown side by side (figure modified after Streck and others [1999] and Streck and Ferns [2004]) (43.659404, -118.998954 WGS84 geographic coordinates; 4835986mE, 338820mN WGS84 UTM Zone 11 coordinates). Scale bar in upper photograph is 1 m (3.3 ft) high; scale bar in lower photograph is 22 m (72.2 ft) high. Both photographs taken from U.S. Highway 395 looking west-southwest.

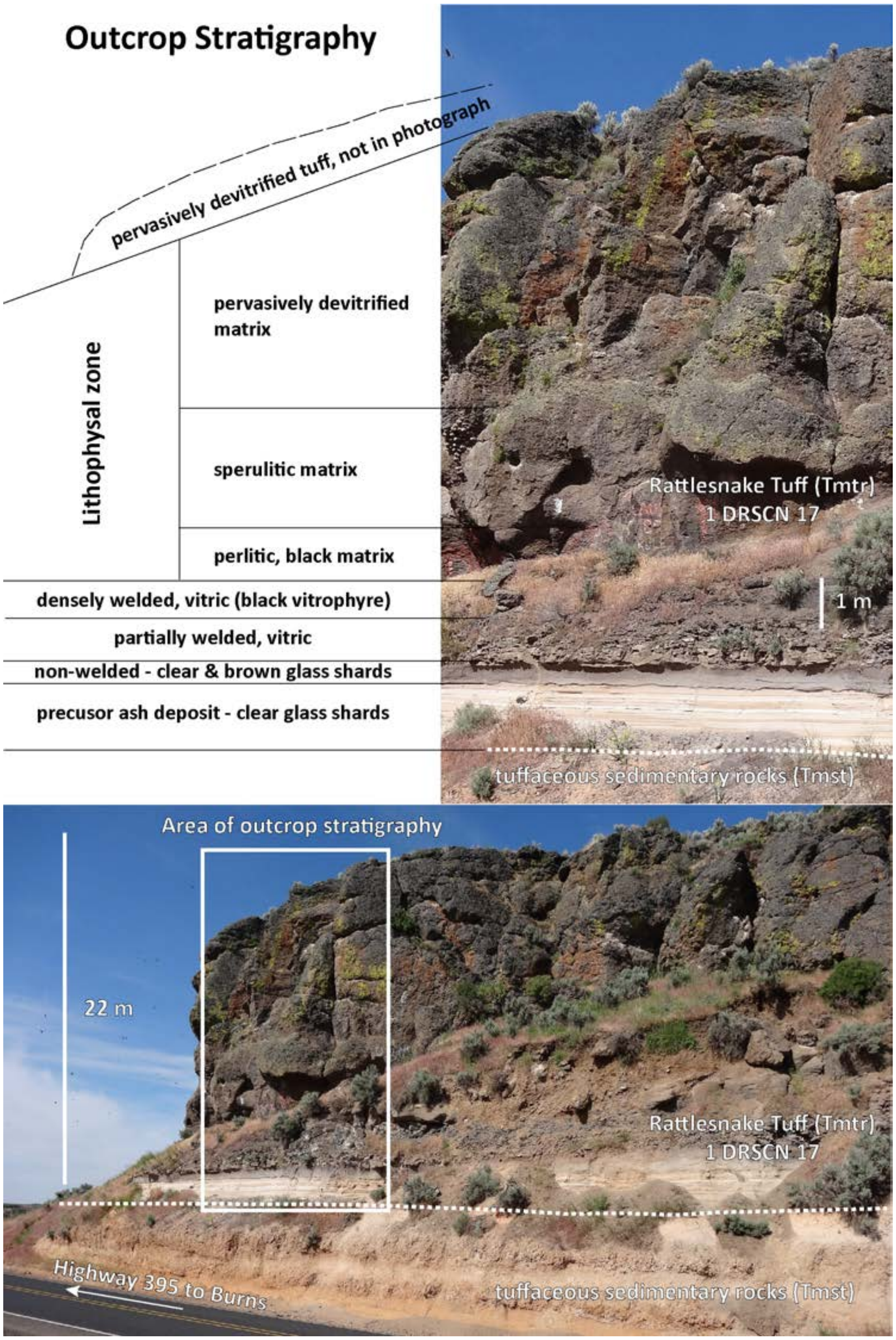

Table 5-1. Representative XRF analyses for early to middle Miocene volcanic rocks in the Devine Ridge South 7.5′ quadrangle. A separate digital Microsoft Excel® spreadsheet (DRS2018_DATA.xlsx) tabulates the 50 geochemical analyses of the volcanic rocks sampled for this study.

Sample No.	HAH147-16	36 DRSCN 17	147 DRSCN 17	53 DRSCN 17	81 DRSCN 17	96 DRSCN 17	21 DRSCN 17	101 DRSCN 17
Formation	Rattlesnake Tuff	Prater Creek Ash-flow Tuff	Devine Canyon Ash-flow Tuff	Dinner Creek Tuff	N/A	N/A	N/A	N/A
Map_Unit	Rattlesnake Tuff	Prater Creek Ash-flow Tuff	Devine Canyon Ash-flow Tuff	Dinner Creek Tuff	basalt-basaltic andesite	andesite	dacite	rhyolite
Map Label	Tmtr	Tmtp	Tmtd	Tmdc	Tmb	Toa	Toda	Tor
UTM N (NAD83)	4839019	4844529	4844895	4855177	4851904	4845514	4845170	4845708
UTM E (NAD83)	350233	346443	343162	347882	348851	347075	344091	347830
Age (Ma)	7.05	8.41	9.63	~16	nd	24.75	nd	nd
Map No.	outside map area	G12	G20	G29	G30	G39	G28	G45
Oxides, weight percent								
SiO_2	76.99	76.50	77.40	76.25	53.64	59.85	64.58	72.33
Al_2O_3	12.23	11.86	11.06	13.40	13.67	17.19	16.54	14.21
TiO_2	0.16	0.15	0.20	0.24	2.28	0.85	0.60	0.47
FeO*	1.53	2.27	2.96	1.53	13.22	6.21	4.55	3.93
MnO	0.07	0.03	0.04	0.03	0.26	0.13	0.07	0.02
CaO	0.19	0.20	0.12	0.50	8.23	6.57	4.95	3.52
MgO	0.16	0.10	0.03	0.08	3.61	3.42	2.38	0.53
K_2O	4.51	4.57	4.80	3.66	1.59	1.76	2.45	1.77
Na_2O	4.15	4.31	3.39	4.30	3.13	3.75	3.61	3.07
P_2O_5	0.02	0.02	0.01	0.02	0.38	0.28	0.26	0.15
Total I	98.52	98.52	96.83	98.08	97	97.99	98.06	95.92
LOI	0.69	0.69	2.56	1.04	2.21	1.2	1.44	3.38
Trace elements, parts per million								
Ni	3	4	4	8	15	44	30	22
Cr	4	2	4	5	5	28	42	41
Sc	4	2	1	6	37	18	12	9
V	6	8	8	16	436	149	98	51
Ba	639	173	56	1432	610	1009	1220	1056
Rb	92	103	122	75	35	53	47	29
Sr	13	13	9	37	341	595	619	428
Zr	304	495	1005	454	174	130	124	102
Y	83	66	117	93	39	17	14	10
Nb	30.8	44.6	73.6	24.9	10.6	7.2	7.5	4.5
Ga	20	22	27	23	20	19	18	14
Cu	5	5	7	6	83	66	53	28
Zn	87	100	201	85	126	74	70	45
Pb	18	19	27	15	7	10	10	11
La	38	60	73	48	20	19	24	15
Ce	77	78	150	81	44	43	46	31
Th	8	9	13	8	4	2	4	5
Nd	47	52	73	53	25	18	20	15
U	4	3	5	4	2	2	2	1

Major element determinations have been normalized to a 100-percent total on a volatile-free basis and recalculated with total iron expressed as FeO*; nd is no data or element not analyzed; na is not applicable or no information; Total I is total initial unnormalized major elements weight percent; LOI is loss on ignition. *Table includes comparable analysis of the Rattlesnake Tuff from adjacent Harney 7.5′ quadrangle (R. A. Houston and others, unpub. data, 2016).

Tmtp **Prater Creek Ash-flow Tuff (upper Miocene)**—Devitrified, welded, crystal-poor ash-flow tuff forming prominent cliff exposures in the western and northern parts of the quadrangle (Plate 1). The tuff is massive, densely welded, and exhibits a eutaxitic texture often parallel to either lobate-platy jointing or distinctive platy jointing. In the map area the Prater Creek Ash-flow Tuff is approximately 10 to 20 m (32 to 65 ft) thick and occurs as a single cooling unit. Walker (1979) designated a type section for the Prater Creek Ash-flow Tuff (**Tmtp**) in the Devine Ridge South 7.5′ quadrangle along the walls of Poison Canyon as shown in **Figure 5-3A**.

Typical hand samples are pinkish gray (5YR 8/1) to light brown (5YR 5/2) and contain rare crystal fragments of sanidine and quartz < 0.5 mm (0.01 in) held in an ash groundmass (**Figure 5-3B**). Also, hand samples contain 2 to 3 cm (0.8 to 1.2 in) or smaller lithophysae; the larger are usually filled. Abundant flattened pumice (fiamme) range from millimeters up to 5 cm (2 in.) in length with a compaction ratio of 10:1. Lithics are minor (5 percent by volume) and consist of poly-compositional angular fragments up to 2 cm (0.78 in) long. In thin section, the tuff is characterized by less than 1 percent sanidine and quartz crystal fragments in a devitrified glass-shard groundmass. Locally, flattened pumice has been zeolitized.

The 16 samples obtained from Prater Creek Ash-flow Tuff (**Tmtp**) in the study area are rhyolitic in composition with 76.45 to 76.77 weight percent SiO_2, 11.62 to 12.14 weight percent Al_2O_3, 4.01 to 4.44 weight percent Na_2O, and 4.51 to 4.64 weight percent K_2O. The tuff also contains a range of barium (70 to 408 ppm Ba), zirconium (476 to 508 ppm Zr), yttrium (35 to 102 ppm Y), and niobium (42.3 to 46.2 ppm Nb) (**Table 5-1; Figure 5-4**; **Figure 5-5**). The Prater Creek Ash-Flow Tuff has reversed magnetic polarity and is assigned a late Miocene age on the basis of an $^{40}Ar/^{39}Ar$ age of 8.41 ± 0.16 Ma (Jordan and others, 2004). The Prater Creek Ash-Flow Tuff has an estimated eruptive volume of ~200 km^3 (48 $mile^3$; Parker, 1974).

Figure 5-3. Field photograph of the Prater Creek Ash-flow Tuff (Tmtp). (A) The Prater Ash-flow Tuff, 7 to 8 mi (11 to 12 km) north of Burns, along the west side of U.S. Highway 395. The upper ledge, at skyline, is the welded part of the Rattlesnake Tuff (Tmtr). Tuffaceous sedimentary rocks (unit Tmst) underlie the Prater Creek Ash-flow Tuff (Tmtp). Photograph taken from U.S. Highway 395 looking west. (43.676596, -118.999331 WGS84 geographic coordinates; 4837896mE, 338836mN WGS84 UTM Zone 11 coordinates). Scale bar is 12 m (39.4 ft) high. (B) In hand sample, the devitrified welded groundmass contains fiamme (arrow), lithic fragments, and rare alkali feldspar crystals (43.741265, -118.914546 WGS84 geographic coordinates; 4844918mE, 345836mN WGS84 UTM Zone 11 coordinates). Sample number: 28 DRSCN 17.

Figure 5-4. Total alkali ($Na_2O + K_2O$) vs. silica (SiO_2) plot classification (TAS), showing whole-rock XRF analyses of middle Miocene to upper Oligocene volcanic rocks in the Devine Ridge South 7.5′ quadrangle (normalized to 100 percent anhydrous). TAS graph fields are from Le Bas and others (1986) and Le Maitre and others (1989).

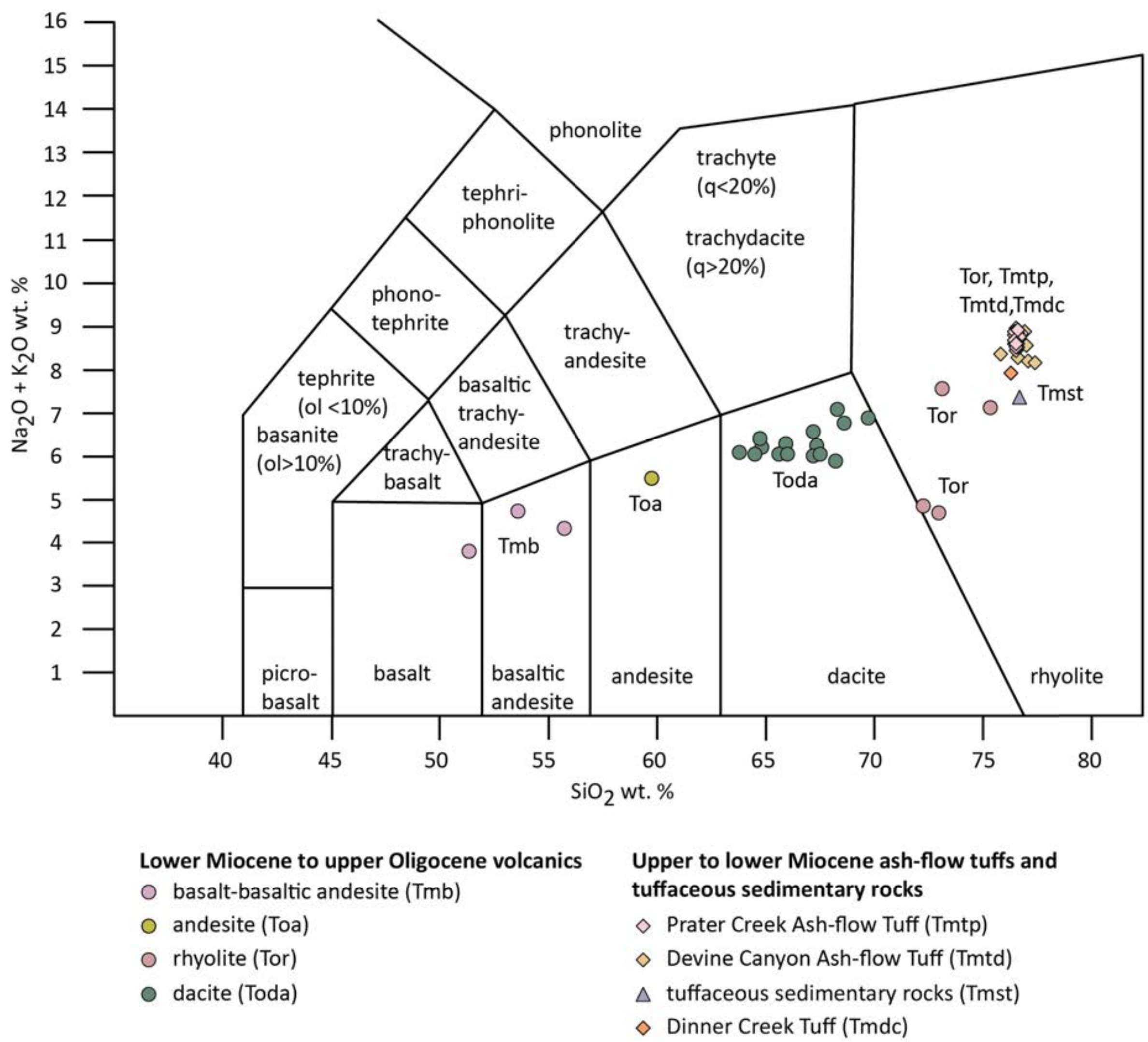

Figure 5-5. Variation diagram showing niobium (Nb) versus zircon (Zr) for units Tmdc, Tmtd, Tmtp, and Tmtr.

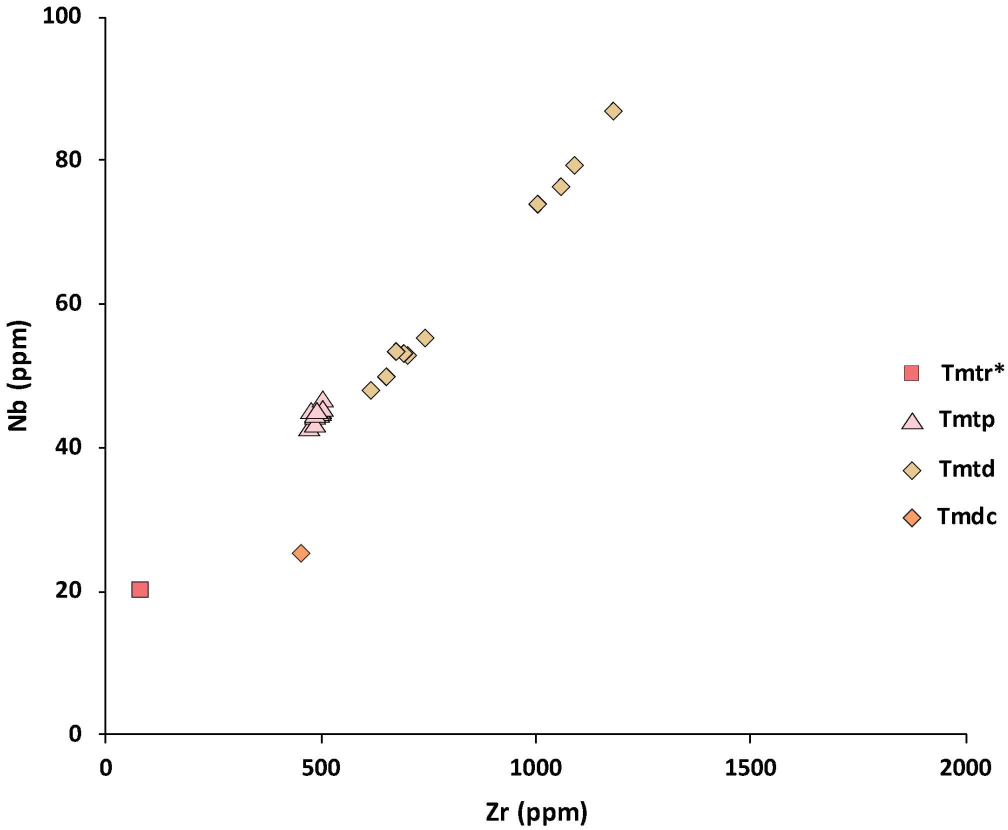

* Tmtr is a representative sample of Rattlesnake Tuff. Tmtp is Prater Creek Ash-flow Tuff. Tmtd is Devine Canyon Ash-flow Tuff. Tmdc is Dinner Creek Tuff.

Tmtd **Devine Canyon Ash-flow Tuff (upper Miocene)**—Crystal-rich vitric tuff forming prominent cliff exposures in the northeastern parts of the quadrangle (**Figure 5-6A; Plate 1**). Densely welded zones weather to form distinctive aprons of very large (up to 10 m diameter; 30 ft) boulders. Another feature of the unit is formation of pavement outcrop. Within the study area, unit thicknesses of 10 m (30 ft) are typical.

Recognition of this tuff in the field is by its abundantly alkali feldspar porphyritic texture (**Figure 5-6B**). The tuff weathers to produce feldspar-rich detritus, which flashes in sunlight and is useful to map the unit in areas of poor exposure. Typically, hand samples of the ash-flow tuff are light gray (N7 to N8) to greenish gray (5GY 5-6/1). Petrographically, the tuff contains as much as 30 percent crystals and crystal fragments of dominantly alkali feldspar (sanidine [Greene, 1973; Smith and MacKenzie, 1958]) minor quartz, and rare pyroxene, ilmenite, and magnetite. Greene (1973) noted that alkali feldspar and quartz generally increase in abundance up section. Most of the phenocrysts are broken and exhibit rounding or resorption embayment textures. Rare pyroxene phenocrysts are green and yellow green (pleochroic) in color.

The 10 samples obtained from the Devine Canyon Ash-flow Tuff (**Tmtd**) in the study area have a rhyolitic geochemical composition of 75.84 to 77.4 weight percent SiO_2, 10.8 to 11.68 weight percent Al_2O_3, 3.08 to 4.04 weight percent Na_2O, and 4.42 to 5.49 weight percent K_2O. These samples also contain 41 to 208 ppm of barium (Ba), 619 to 1,184 ppm of zirconium (Zr), 47 to

165 ppm of yttrium (Y), and 48.0 to 86.9 ppm of niobium (Nb) (**Table 5-1; Figure 5-4**; **Figure 5-5**). The range in zirconium, yttrium, and niobium suggests the tuff was erupted from a geochemically zoned magma chamber (Isom 2017). The unit is assigned a late Miocene age on the basis of stratigraphic position and an $^{40}Ar/^{39}Ar$ age of 9.63 ± 0.05 Ma (Ford and others, 2013). The Devine Canyon Ash-flow Tuff (**Tmtd**) is believed to have covered more than 18,600 km^2 (7,200 mi^2) with a total erupted volume of approximately 195 km^3 (47 mi^3) (Greene, 1973). Eruptive sources for the tuff are suggested to lie within the Harney Basin (Greene, 1973; Parker, 1974). The unit is equivalent to the welded tuff of Devine Canyon of Greene (1973).

Figure 5-6. Outcrop and petrographic description of the Devine Canyon Ash-flow Tuff (Tmtd) exposed in the northeastern parts of the map area. (A) Cliff exposure (43.719452, -118.885894 WGS84 geographic coordinates; 4842442mE, 348088mN WGS84 UTM Zone 11 coordinates). Sample number: 306 DRSCN 17. View looking north. (B) Stony(?) devitrified tuff with lithic fragment (arrow). (43.734760, -118.889201 WGS84 geographic coordinates; 4844148mE, 347861mN WGS84 UTM Zone 11 coordinates). Hammer for scale, scale bar is 10 cm (4 in) high. Sample number: 44 DRSCN 17.

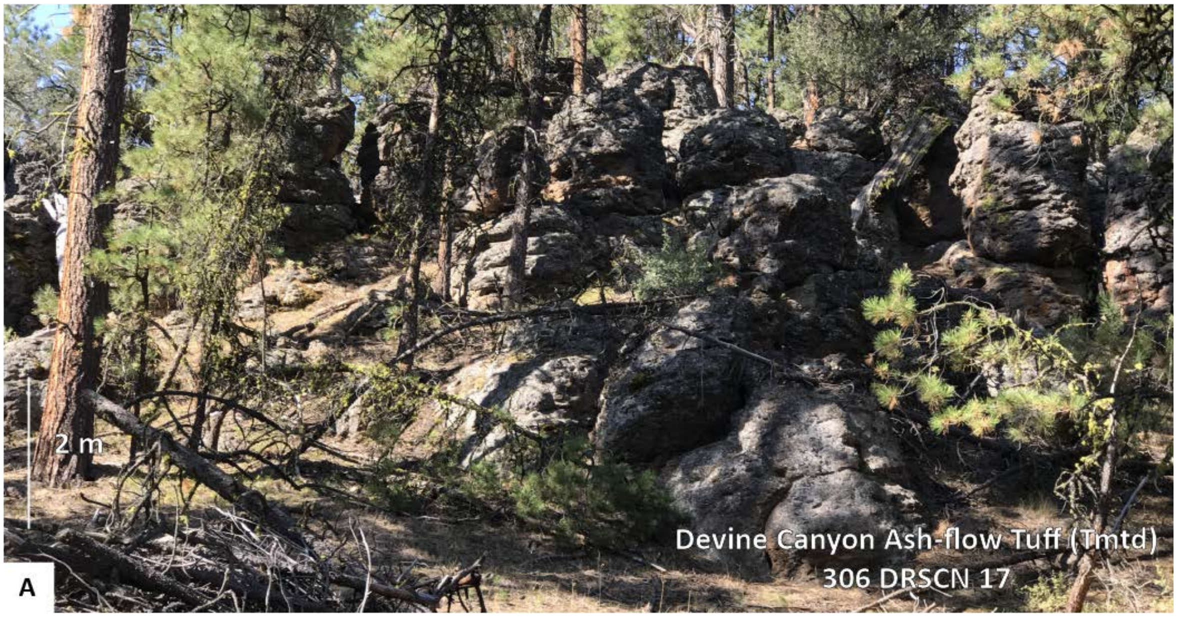

Tmst **tuffaceous sedimentary rocks (upper Miocene[?] and middle Miocene[?])**—tuffaceous mudstone, siltstone, sandstone, and conglomerate sedimentary rocks and associated fluvial reworked tuff (**Figure 5-7**). Includes all sedimentary rocks between and separating the Rattlesnake Tuff (**Tmtr**) and Prater Creek Ash-flow Tuff (**Tmtp**), **Tmtp** and Devine Canyon Ash-flow Tuff (**Tmtd**), and beneath **Tmtd** (**Figure 5-1**). **Tmst** is interpreted by the authors as being interbedded with the tuffs. Because of this interpretation, the three intervals of **Tmst** are not mapped individually. **Tmst** has a maximum exposed thickness of about 137 m (450 ft) along the western boundary of the study area.

Paleotopography had a marked effect on the deposition and distribution, e.g., pinch-outs, along with the lateral extent of the tuffs in places. Although differential weathering is probably responsible for much of the paleotopography, the effects of faulting are important especially in the northeastern part of the study area.

From stratigraphic relationships and age dates on bracketing tuff marker beds, the unit is assigned a middle to late Miocene age.

Tmst is partially equivalent lithologically to the following:

- Td (Danforth Formation) of Piper and others (1939);
- Tst (sedimentary rocks) of Greene (1972);
- Tst (tuffaceous sedimentary rocks) of Greene and others (1972);
- Sedimentary rocks of Tdv (welded tuff of Devine Canyon) of Greene (1972);
- Tst (tuffaceous sedimentary rocks and tuff) of Walker (1977); and
- Tmst-1, -2, and -3 (tuffaceous sedimentary rocks) of Brown and others (1980).

Figure 5-7. View of the tuffaceous sedimentary rocks (Tmst). A sequence of the tuffaceous sedimentary rocks (Tmst) between prominent cliffs of the overlying Rattlesnake Tuff (Tmtr) and the underlying Prater Creek Ash-flow Tuff (unit Tmtp). View is looking north toward the mouth of Gradon Canyon. Truck is parked next to Poison Creek (arrow indicates creek flow direction). The scale bar is 3 m (9 ft) in length (43.676596, -118.999331 WGS84 geographic coordinates; 4837896mE, 338836mN WGS84 UTM Zone 11 coordinates).

Nonconformity

5.3.3 Middle to lower Miocene volcanic rocks

Tmdc **Dinner Creek Tuff (middle Miocene or lower Miocene)**—Massive, crystal poor, pumice and lithic rich, moderately to densely welded rhyolitic ash-flow tuff recognized at only one location in the northeast part of the map area. It exists only as scattered boulder float. The tuff commonly has a brown-purple devitrified ash groundmass. Pinkish light gray tuff contains white pumice and lithic fragments up to 3 cm (1 in) in diameter (**Figure 5-8A**). The pumice fragments do not exhibit textures related to compaction. Although the tuff is poorly exposed in map area and in the Harney and Devine Ridge North 7.5′ quadrangle area, R. A. Houston and others (unpub. data, 2017) estimate the tuff thickness there to range from 10 to 20 m (32 to 65 ft). In hand sample, the tuff contains angular light gray (N8 to N7) pumice up to 2 cm (0.75 in), minor lithic fragments and sparse, < 5 percent, angular fragments of anhedral plagioclase and clinopyroxene and minor quartz up to 2 mm (0.08 in) in length (**Figure 5-8B**). A sample obtained from Dinner Creek Tuff (**Tmdc**) in the study area has a rhyolitic whole-rock chemical composition of 76.25 weight percent SiO_2, 13.4 weight percent Al_2O_3, 4.3 weight percent Na_2O, and 3.66 weight percent K_2O (**Table 5-1; Figure 5-4**; **Figure 5-5**). The sample of **Tmdc** also contains 1,432 ppm of barium (Ba), 454 ppm of zirconium (Zr), 93 ppm of yttrium (Y), and 25.0 ppm of niobium (Nb). The unit is equivalent to Dinner Creek Welded Ash-flow Tuff of Kittleman and others (1965); Dinner Creek Welded Tuff of Greene and others (1972); Dinner Creek Tuff of Ferns and others (1993); and the Dinner Creek Tuff of Streck and others (2015). The unit is middle or early Miocene based on stratigraphic position and because of $^{40}Ar/^{39}Ar$ ages of 15.9 ± 0.09 Ma and 16.16 ± 0.02 Ma obtained by Streck and others (2015).

Figure 5-8. Dinner Creek Tuff (Tmdc) float. (A) Pumice rich welded tuff with two pumice colors (arrow). Hammer head for scale is 10.2 cm (4 in) in length (43.744019, -118.889226 WGS84 geographic coordinates; 4845177mE, 347882mN WGS84 UTM Zone 11 coordinates) Sample number: 53 DRSCN 17. (B) Pinkish to tan groundmass with brown pumice (arrow) and rounded lithic fragments. U.S. dollar coin for scale, scale bar is 2.65 cm (~1 in) in length. Sample number: 53 DRSCN 17.

Tmb **basalt–basaltic andesite (lower Miocene[?])**—Flow-on-flow succession of aphyric to olivine-, clinopyroxene-, and plagioclase-microporphyritic basalt and basaltic andesite exposed in the northeastern corner of the map area (**Figure 5-9A**) (Plate 1). The unit is positioned stratigraphically beneath Dinner Creek Tuff (**Tmdc**) and above andesite (**Toa**) (**Figure 5-1**). The flows are discontinuous and exposed as rubbly outcrops surrounded by reddish-brown iron-oxidized soils. The total thickness of **Tmb** in the map area is approximately 76 m (250 ft); mapped individual flows outside of the area have thicknesses up to 10 m (32 ft) (R. A. Houston and others, unpub. data, 2016; R. A. Houston and others, unpub. data, 2017).

Hand samples of the basalt-basaltic andesite are medium gray (N5) to pale-red purple (5RP 6/2) containing ~40 to 50 percent subhedral plagioclase laths up to 2 mm (0.08 in) in length (**Figure 5-9B**). In thin section, anhedral clinopyroxene exhibit poikilitic textures and occur up to 30 percent in the sample (**Figure 5-9C, D**). Olivine, commonly altered to iddingsite, in the sample thin section is present up to 10 percent. Geochemical analyses of two of three samples from **Tmb** have a basaltic andesite chemical composition, while the third has a basaltic chemical composition (**Table 5-1; Figure 5-4**). The two basaltic andesite samples contain 53.64 to 55.79 weight percent SiO_2, 13.67 to 16.74 weight percent Al_2O_3, 1.49 to 2.28 weight percent TiO_2, 3.39 to 3.61 weight percent MgO, and 0.34 to 0.38 weight percent P_2O_5. These samples also contain 112 to 174 ppm zirconium (Zr), 29 to 39 ppm yttrium (Y), and 6.5 to 10.6 ppm niobium (Nb). The sample of basalt contains 51.33 weight percent SiO_2, 13.91 weight percent Al_2O_3, 2.27 weight percent TiO_2, 4.63 weight percent MgO, and 0.32 weight percent P_2O_5. This basalt sample also contains 103 ppm zirconium (Zr), 45 ppm yttrium (Y), and 5.0 ppm niobium (Nb). The unit is assigned an early Miocene age on the basis of stratigraphic position.

Figure 5-9. Basalt-basaltic andesite (Tmb). (A) Aphyric to olivine-, clinopyroxene-, and plagioclase-microporphyritic basalt-basaltic andesite exposed as rubbly outcrop. Hammer for scale (arrow points to hammer; 28 cm [11 in] length); scale bar is 1 m (3.3. ft) tall. (43.744344, -118.877204 WGS84 geographic coordinates; 4845191mE, 348851mN UTM Zone 11 coordinates). Sample number: 81 DRSCN 17. *(Figure continued on following pages.)*

(Figure 5-9, continued) **Basalt-basaltic andesite (Tmb). (B) Medium gray (N5) to pale-red purple (5RP 6/2) containing ~40 to 50 percent subhedral plagioclase laths up to 2 mm (0.08 in) in length. U.S. dollar coin for scale, 2.65 cm (~1 in) in diameter; scale bar is 2.65 cm (~1 in) (43.744344, -118.877204 WGS84 geographic coordinates; 4845191mE, 348851mN UTM Zone 11 coordinates). Sample number: 81 DRSCN 17.**

(Figure 5-9, continued) **Basalt-basaltic andesite (Tmb). (C) A photomicrograph of 50 percent plagioclase crystals and up to 30 percent anhedral clinopyroxene (plane-polarized light). The clinopyroxenes exhibit a poikilitic textures. Opaque minerals constitute less than 3 percent by volume. Scale bar is 1 mm (0.04 in) in length. Sample number: 81 DRSCN 17. (D) Same view as (C) under cross-polarized light. Sample number: 81 DRSCN 17.**

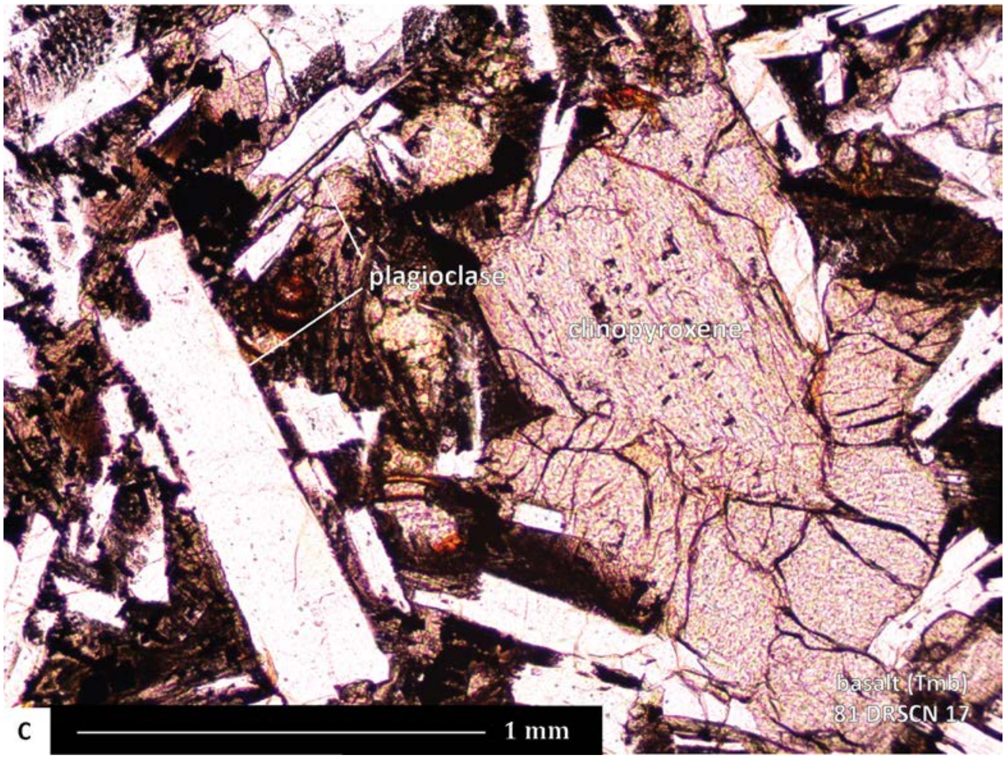

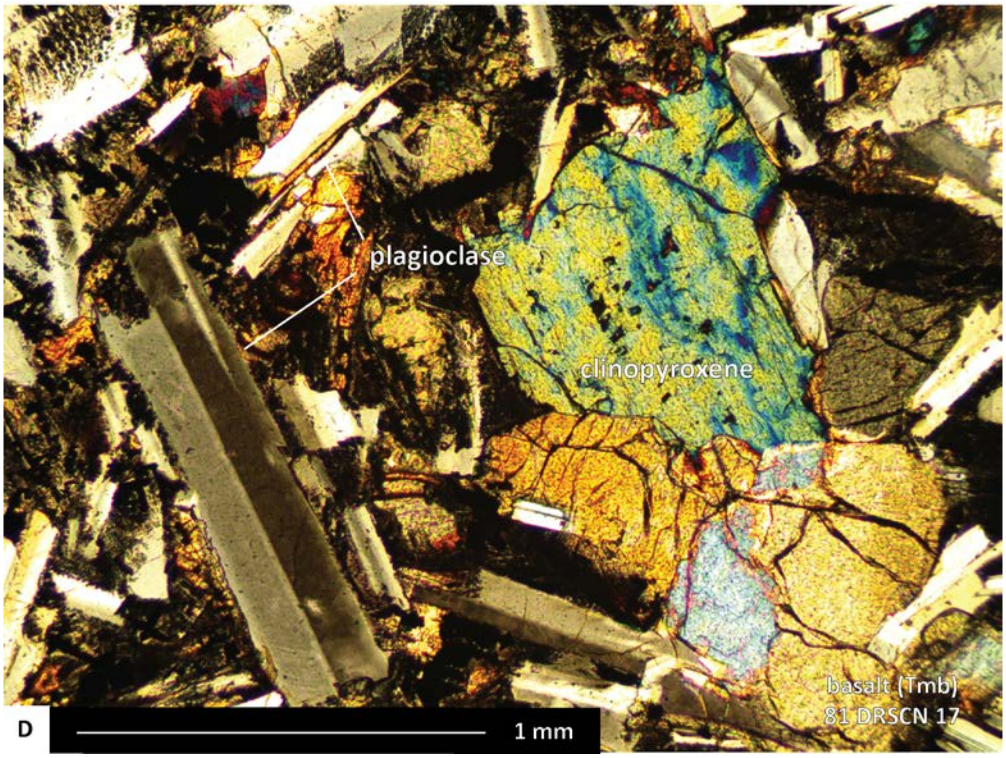

Angular unconformity to disconformity

5.3.4 Upper Oligocene volcanic rocks

Toa **andesite (upper Oligocene)**—Plagioclase, biotite, clinopyroxene andesite (**Toa**) exposed as float in the northern part of the study area (**Figure 5-10A;** Plate 1). The float is scattered and spread on the sides of a rounded hill and is exposed nowhere else in the map area. Thickness of the unit is unknown, but collectively, in the adjoining Harney and Devine Ridge North 7.5′ quadrangles (R. A. Houston and others, unpub. data, 2016; R. A. Houston and others, unpub. data, 2017), the total exposed thickness is up to 76 m (250 ft). In hand sample, the andesite is medium gray (N5) and contains ~60 percent subhedral plagioclase laths up to 1 mm (0.04 in) in length (**Figure 10B**). Petrographically, the rock contains plagioclase and clinopyroxene phenocrysts and biotite within a groundmass of feldspar microlites (**Figure 10C, D**). A sample obtained for this unit has an andesitic chemical composition of 59.85 weight percent SiO_2, 17.19 weight percent Al_2O_3, 0.85 weight percent TiO_2, 3.42 weight percent MgO, and 0.28 weight percent P_2O_5. This sample also contains 130 ppm of zirconium (Zr), 17 ppm yttrium (Y), and 7 ppm niobium (Nb) (**Table 5-1; Figure 5-4**). **Toa** has a reversed magnetic polarity and is assigned a late Oligocene age based on stratigraphic position and an $^{40}Ar/^{39}Ar$ age of 24.75 ± 0.15 Ma (R. A. Houston and others, unpub. data, 2016; R. A. Houston and others, unpub. data, 2017).

Figure 5-10. Andesite (Toa). (A) Float boulders of andesite exposed near the top of a dome-shaped hill. Hammer for scale (arrow points to hammer; 41 cm [16 in] length); scale bar is 1 m (3.3 ft) tall (43.746890, -118.899344 WGS84 geographic coordinates; 4845514mE, 347075mN WGS84 UTM Zone 11 coordinates). Sample number: 96 DRSCN 17. *(Figure continued on following pages.)*

(Figure 5-10, continued) **Andesite (Toa). (B) Hand sample of andesite containing minor subhedral plagioclase laths surround by a fine-grained, microporphyritic groundmass. U.S. dollar coin for scale; scale bar is 2.65 cm (~ 1 in). Sample number: 96 DRSCN 17.** *(Figure continued on following pages.)*

(Figure 5-10, continued) **Andesite (Toa). (C) Photomicrograph of andesite showing characteristic porphyritic and glomeroporphyritic textures (plane-polarized light). The large plagioclase phenocryst is zoned and twinned. Opaque minerals/glass constitute less than 5 to 10 percent by volume. Scale bar is 1 mm (0.04 in) in length. Sample number: 96 DRSCN 17.** *(Figure continued on following page.)*

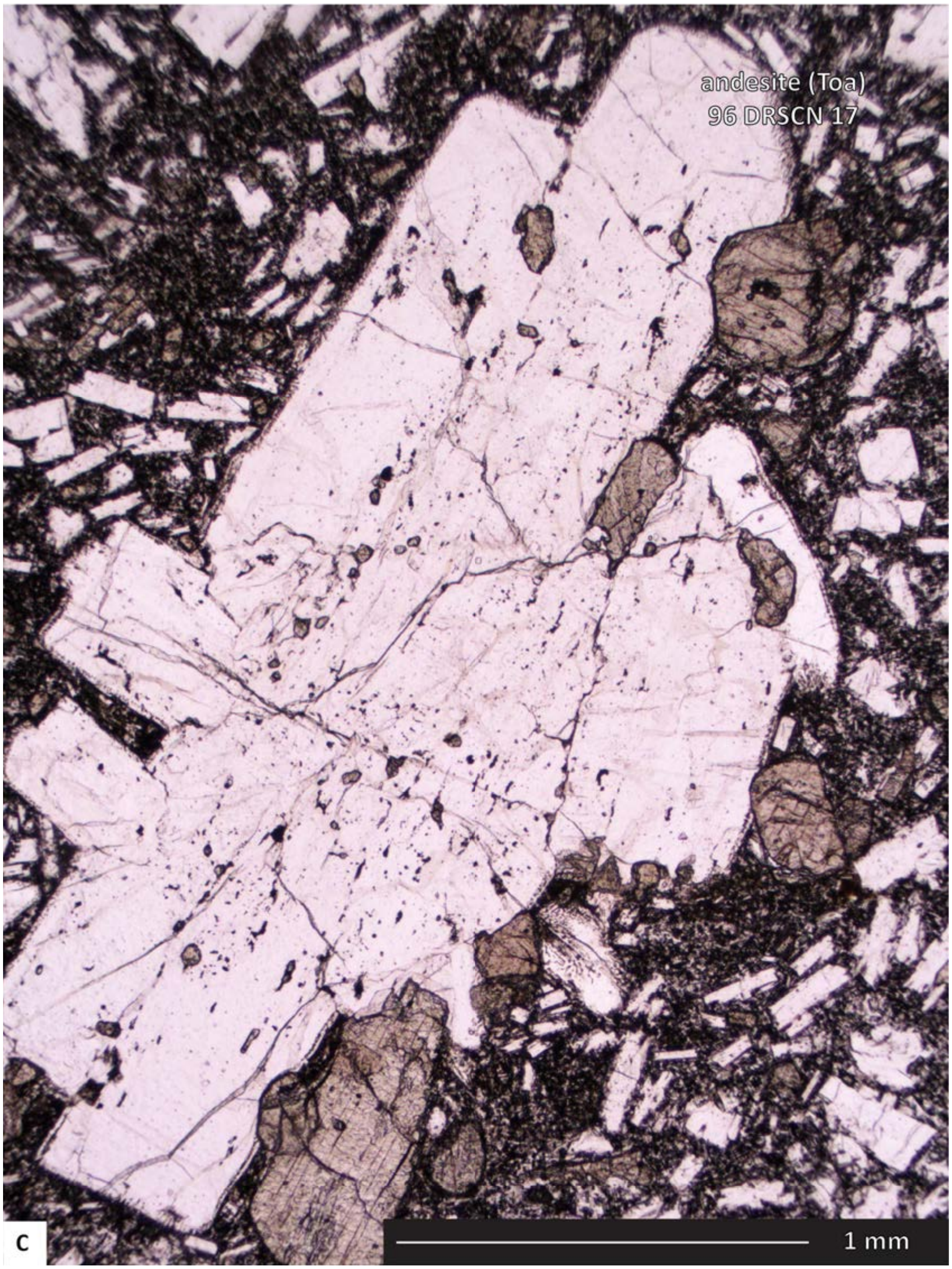

(Figure 5-10, continued) **Andesite (Toa). (D) Same view as (C) under cross-polarized light. Sample number: 96 DRSCN 17.**

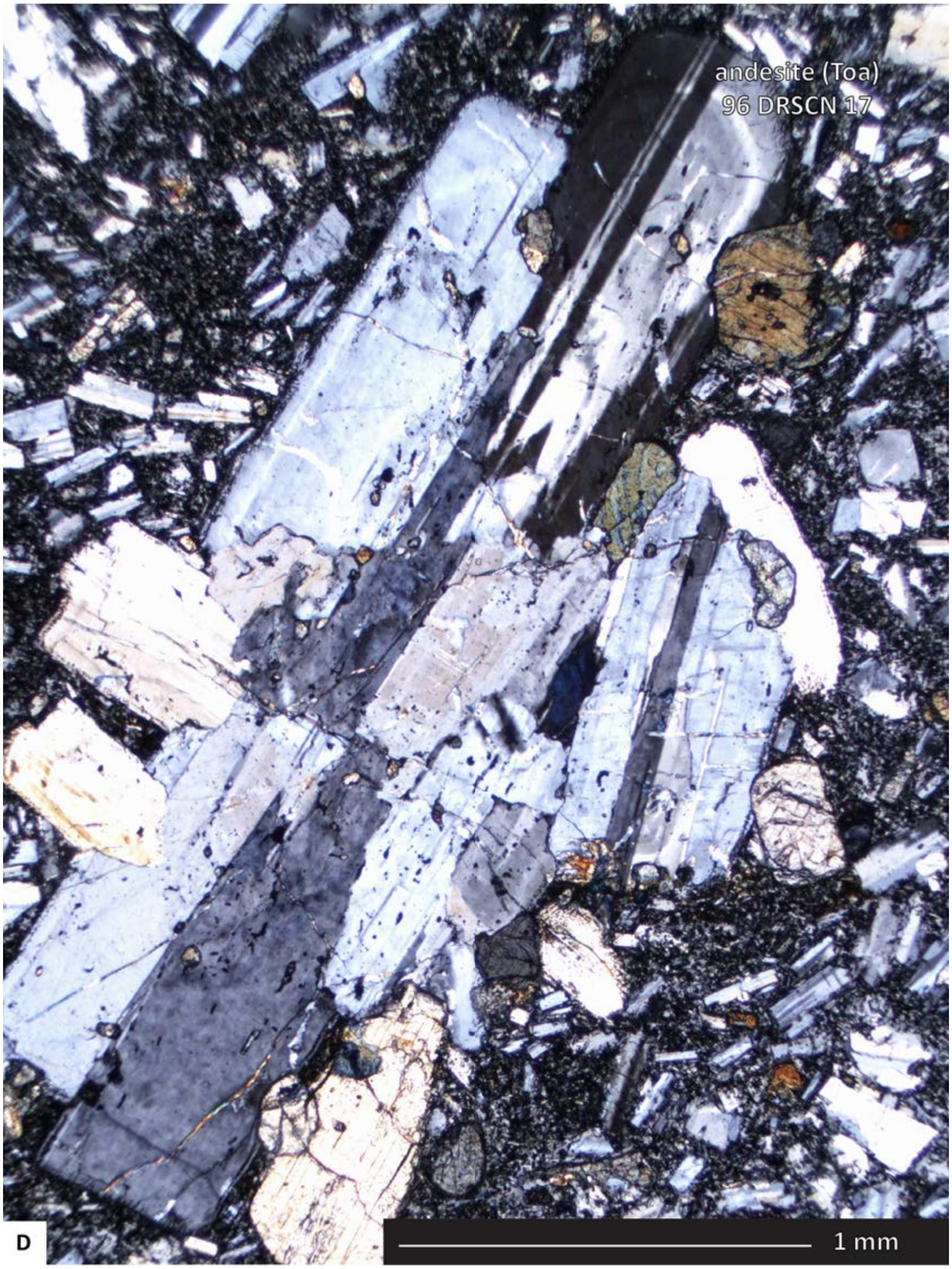

Tor **rhyolite (upper Oligocene[?])**—Quartz-sanidine rhyolite dikes and plug-like bodies (**Tor**) are exposed in the northeastern part of the map area (**Figure 5-11A**; Plate 1). Three plug-like bodies measuring 15 m to 25 m (49 ft to 82 ft) across are exposed on the ridge just east of Miller Creek (Plate 1). Several smaller rhyolitic dikes, measuring less than 10 meters (98 ft) in width and about twice as long cut a hillside to the northwest along Soldier Creek (Plate 1). This and the rhyolite plugs intrude the dacite of unit **Toda**. Hand samples of the rhyolite vary in color and texture. The plugs are characterized by a very fine grained, light to medium light gray (N7 to N6) to pinkish groundmass (**Figure 5-11B**). They are slightly to moderately porphyritic and are flow banded. Petrologic investigations reveal subhedral to euhedral and embayed quartz phenocrysts ranging in size from 0.5 to 1.5 mm (0.02 to 0.06 in) (**Figure 5-11C**).

The four rhyolite samples obtained from **Tor** contain 72.33 to 75.4 weight percent SiO_2, 13.61 to 14.62 weight percent Al_2O_3, 0.28 to 0.51 weight percent TiO_2, 0.19 to 0.53 weight percent MgO, and 0.06 to 0.15 weight percent P_2O_5. These samples also contain 97 to 185 ppm zirconium (Zr), 9 to 18 ppm yttrium (Y), and 4.5 to 11.4 ppm niobium (Nb) (**Table 5-1; Figure 5-4**). The rhyolite plug-like bodies are silicified, containing numerous chalcedony filled fractures, McGrane (1985) noted that both rhyolitic and quartz porphyry dikes are spatially, temporally, and genetically related to the epithermal gold mineralization at the Idol City District. He mapped the southern extent of this mining district to the boundary between Devine Ridge North 7.5′ quadrangle and the study area. The rhyolite is assigned an late Oligocene age on the basis of stratigraphic position.

Figure 5-11. Rhyolite (Tor) in the northeastern part of the study area. (A) Flow banded rhyolite defined by a strong planar fabric. Hammer for scale (arrow points to hammer; 28 cm [11 in] length); scale bar is 1 m (3.3 ft) tall (43.45386, -118.884217 WGS84 geographic coordinates; 4845385mE, 348260mN WGS84 UTM Zone 11 coordinates). Looking northwest. Sample number: 69 DRSCN 17. *(Figure continued on following page.)*

(Figure 5-11, continued) **Rhyolite (Tor) in the northeastern part of the study area. (B) A sequence of banding accentuated by surficial weathering of iron oxide, separated by parallel laminae. Banding displays autoclastic brecciation. Pick tip for scale; scale bar is 2.65 cm (~1 in) in length. (43.740551, -118.878013 WGS84 geographic coordinates; 4844771mE, 348776mN WGS84 UTM Zone 11 coordinates). Sample number: 154 DRSCN 17. (C) Photomicrograph of sample 154 DRSCN 17 that displays a flow texture deflected by a phenocryst. Plane-polarized light. Scale bar is 2 mm (0.08 in) in length. Sample number: 154 DRSCN 17.**

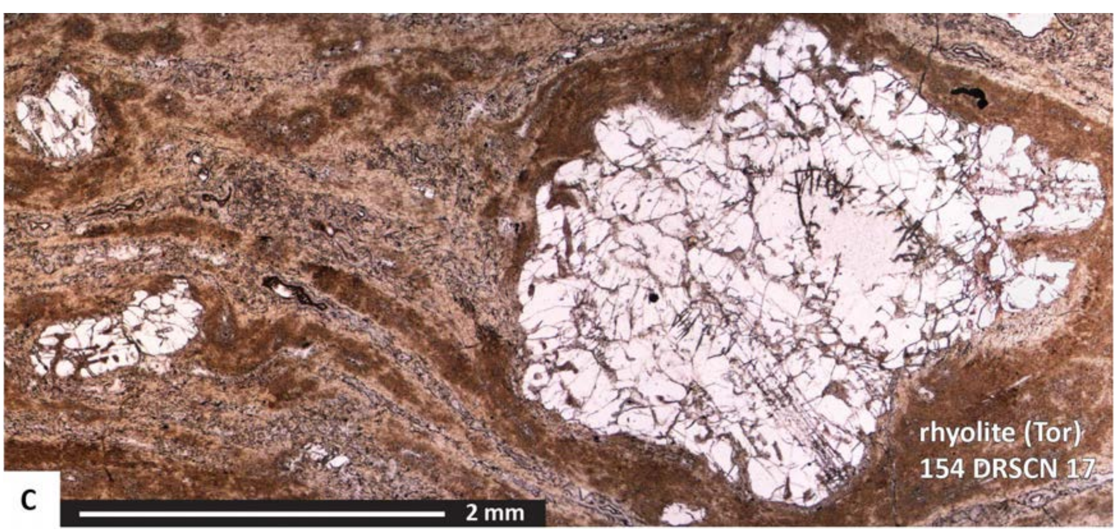

Toda **dacite (upper Oligocene[?])**—Plagioclase- and quartz-phyric dacite is exposed in the north-central and northeastern part of the map area (**Figure 5-12A;** Plate 1). Dacite lava flows (**Toda**) are the oldest rocks in the study area and are overlain by basalt (**Tmb**), andesite (**Toa**), and Devine Canyon Ash-flow Tuff (**Tmtd**). Although the stratigraphic relationship between the dacite (**Toda**) and overlying rocks is clear, the thicknesses of individual dacite flows in the study area are not. However, R. A. Houston and others (unpub. data, 2017) indicated the thickness of flows ranges from 5 m to 10 m (16 ft to 32 ft) with a collective total exposed thickness up to 20[?] m (64 ft).

The dacite lavas show a variety of mineralogies and textures as well as the effects of hydrothermal alteration. Typical hand samples of the dacite are dark gray (N3) and contain ~25 percent plagioclase laths ~5 mm (0.19 in) and minor quartz (<1 mm) set in a fine-grained groundmass. Other varieties include a maroon, hornblende dacite, a light gray-green, hornblende dacite, and a dark gray vesiculated, porphyritic dacite that commonly show well-developed columnar and large blocky jointing. Petrographic inspection of dacite samples reveals a microcrystalline groundmass of dominantly plagioclase and pyroxene microlites with euhedral to subhedral plagioclase, quartz, hornblende, and clinopyroxene (<1 mm c-axis, 0.02 in) (**Figure 5-12B**, **Figure 5-12C, D**). The 15 samples obtained from **Toda** in the study area have dacitic geochemical compositions ranging from 63.90 to 69.82 weight percent SiO_2, 15.49 to 17.43 weight percent Al_2O_3, 0.42 to 0.74 weight percent TiO_2, 0.47 to 2.38 weight percent MgO, and 0.16 to 0.28 weight percent P2O5(**Table 5-1; Figure 5-4**). These samples also contain 1,020 to 1,615 ppm of barium (Ba), 112 to 155 ppm of zirconium (Zr), 11 to 23 ppm of yttrium (Y), and 5.7 to 9.5 ppm of niobium (Nb).

The dacites have normal magnetic polarity (R. A. Houston and others, unpub. data, 2016; R. A. Houston and others, unpub. data, 2017). This unit is assigned a late Oligocene age based on stratigraphic position.

Figure 5-12. Dacite (Toda). (A) Porphyritic and flow banded. The flow banding thicknesses vary from several centimeters up to a meter and often weather out as spines and rows. The white line follows a trough suspected to be a fault structure. View looking north. Hammer for scale is 41 cm (16 in) in length (43.743912, -118.944994 WGS84 geographic coordinates; 4845269mE, 343391mN WGS84 UTM Zone 11 coordinates). Location number 142 DRSCN 17. (B) Hand sample of 142 DRSCN 17: porphyritic with two size groups of plagioclase phenocrysts; millimeter sized (3 to 5 percent) and 5 mm to 1 cm (0.2 in to 0.4 in) set in a microcrystalline groundmass. The larger plagioclase phenocrysts are visibly zoned and many have pitted interiors. U.S. dollar coin for scale, scale bar is 2.65 cm (~1 in). *(Figure continued on following page.)*

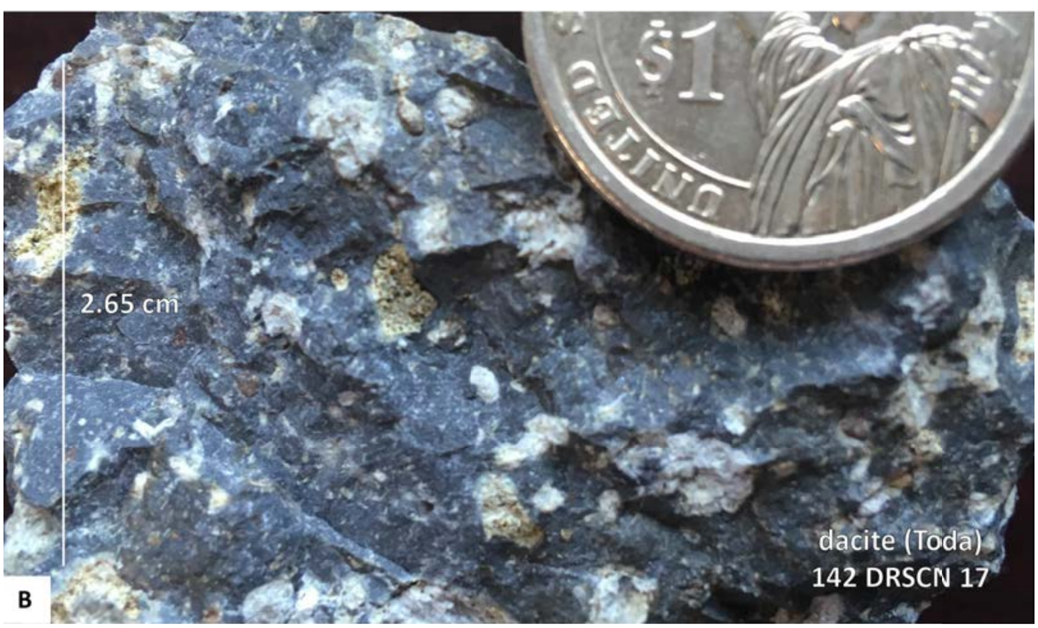

(Figure 5-12, continued) **Dacite (Toda). (C) Photomicrograph of a large plagioclase phenocryst that exhibits two episodes of crystallization, an outer rim and corroded and resorbed inner core (sieve texture). Thin section in plane-polarized light. Scale bar is 1 mm (0.04 in) in length. (D) Same as (C) under cross-polarized light. Scale bar is 1 mm (0.04 in) in length. Sample number: 142 DRSCN 17.**

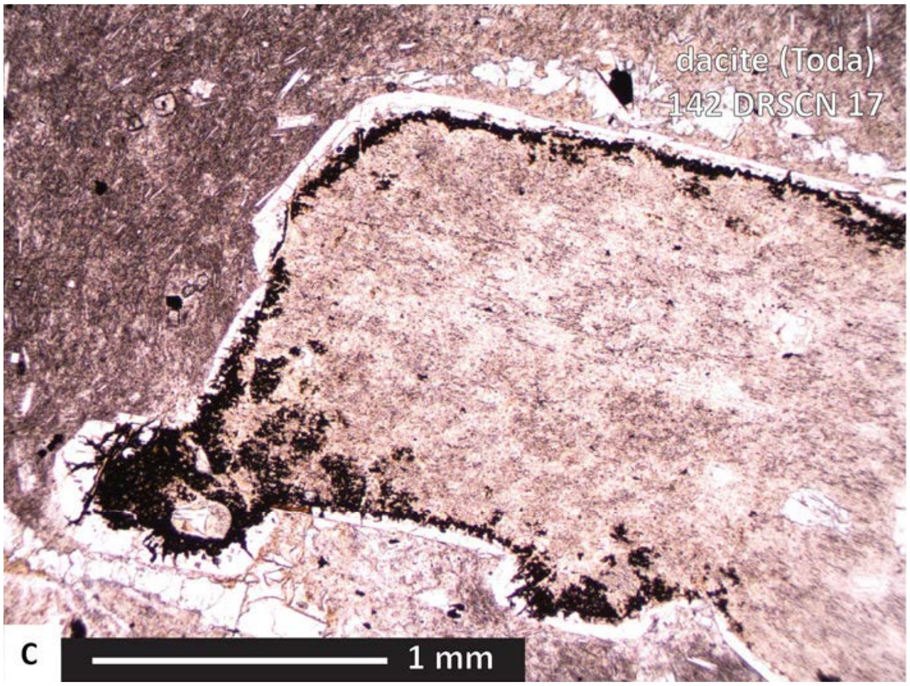

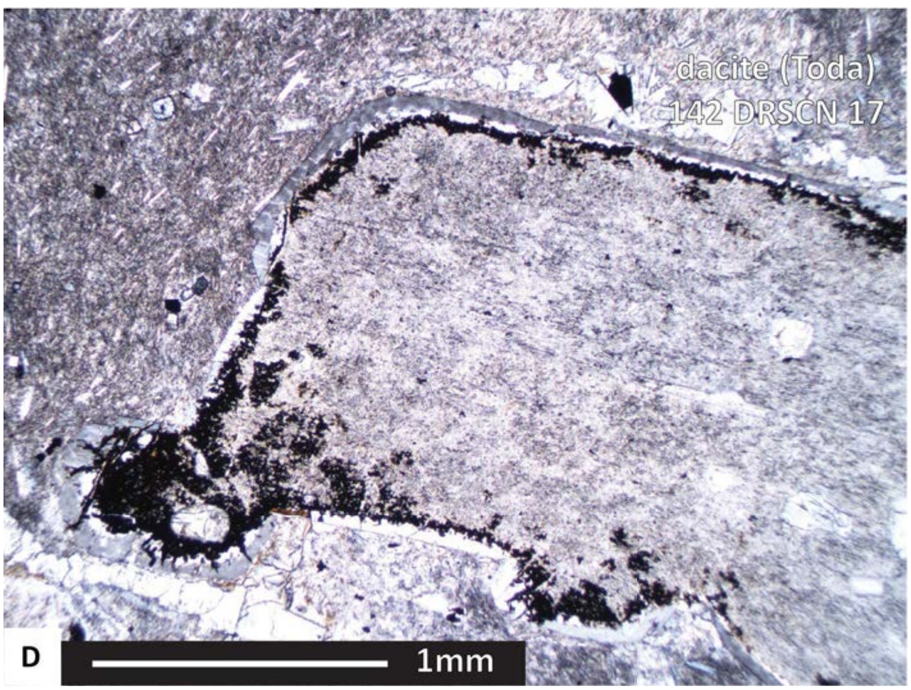

6.0 STRUCTURE

6.1 Introduction

The Devine Ridge South 7.5′ quadrangle is underlain by a generally southward dipping stratigraphic section, wherein the oldest rocks are exposed in the highlands in the north. The depositional sequence both thickens and becomes younger to the south. The stratigraphic section is chopped by a series of faults as described below.

Structure in the map area is defined by the mapped distribution of geologic units, faults, topographic lineaments (as observed in the field, on a 5-m SFM derived DEM, and 2016 NAIP photographs), folds, and bedding attitudes (Plate 1). Primary structural features (e.g., slickensides or fault breccia) are rarely observed in the field. Fault zones, such as those shown on Plate 1, are recognized from the offset between geologic contacts and lithologies, missing units, topographic lineaments as indicators of possible movement, breccia, spring alignment, and subsurface lithologic data obtained from water wells (**Figure 6-1**).

Difficulties recognizing faults in the ash-flow tuffs and tuffaceous sedimentary rocks arise as (1) lateral facies changes in these rocks can be abrupt, (2) fault planes are not expected to be well preserved in moderately weakly indurated strata, (3) those faults observed often have small offsets (less than several centimeters to a meter in some cases) (**Figure 6-1**), (4) separation of beds can be difficult to determine in the field, and (5) areas of distinctly contrasting lithology are rarely exposed.

Additionally, there is the related issue of how to portray small offsets without overexaggerating the apparent offset of strata. On the map plate (Plate 1), where this issue is encountered or the offset is poorly constrained the affected strata are not shown as having an offset. However, interpretations of locations of faults and bed offsets in the map area were improved by using a 5-m SFM derived DEM. Lidar at higher resolution when available will likely result in the identification of more faults with greater accuracy and location confidence.

The northern region of the Harney Basin is cut by a dominant set of steeply dipping, normal and normal oblique northwest-striking faults and by a lesser number of north-striking and east-northeast–striking faults that are interpreted as conjugate Riedel shears. Collectively, faulting has tilted the rocks gently southwest to west-southwest. A major NNW-SSE dextral shear zone referred to herein as the Soldier Creek fault zone bisects the quadrangle. Although these faults cut across all Miocene and Oligocene rocks, they are much less common in the middle Miocene and younger rocks that overlie the more highly deformed late Oligocene dacite (**Toda**). A combination of faulting and some amount of erosion developed a significant paleo-topography prior to the deposition of the 9.6 Ma Devine Canyon Tuff Ash-flow Tuff, determined on the basis of the tuff’s distribution and thickening and thinning of the deposit. Local south to southwest plunging anticlines are recognized in the quadrangle. Faulting and folding appears to have terminated prior to all Quaternary deposits. The following discussion presents the spatial distribution of faults and folds in the quadrangle.

6.2 Faulting in the Devine Ridge South 7.5′ quadrangle

The Soldier Creek fault zone bisects the quadrangle along the west side of the Soldier Creek valley (Brown and others, 1980). The fault continues northward following the Soldier Creek drainage into the adjoining Devine Ridge North 7.5′ quadrangle (Plate 1; **Figure 6-2**). This fault represents a major N-S trending system of oblique-slip faults with right-lateral offset. These faults are likely vertical to subvertical dominantly down to the west. The magnitude of lateral displacement along the faults is difficult to quantify due to poorly defined offset of piercing point.

Mapping along the Soldier Creek fault zone, particularly in the middle reaches of Soldier Creek, identified at least three fault splays (imbricates) along a narrow zone. This zone contains several south facing blocks of ash-flow tuffs (Plate 1; **Figure 6-2**) that appear to be downdropped to the south. These blocks may be the result of duplexing into negative and positive blocks.

The map pattern of units where the cross-section line crosses Soldier Creek shows substantial down-to-the-west displacement of Devine Canyon immediately north of the cross-section line (Plate 1). The map pattern to south shows down-on-the-east displacement against an apparently tilted section of Rattlesnake Tuff (**Tmtr**) over Prater Creek Ash-flow Tuff (**Tmtp**). These apparently contradictory relationships suggest that the Rattlesnake Tuff here wrapped around a topographic high at time of eruption.

Other important structures in the map area are as follows:

- Normal faulting (down on the west) occurs along the eastern side of the Soldier Creek valley (southeastern part of the map area) extending north into Tudor Canyon drainage (Plate 1).
- A concealed fault may mark the valley of Poison Creek slough along U.S. Highway 395 (southwestern part of the map area).
- In the middle of the study area an east-west trending, broad margin or topographic break divides the map area here roughly in half. This margin is where the Prater Ash-flow Tuff (**Tmtp**) not only emerges from various canyon floors across the map area but also coincides with a nearly parallel east-west normal fault (down on the south).
- In the northwest quarter of the map area there are a series of fault blocks formed by northeast-trending normal faults (down on the east).
- A sequence of north-northwest trending faults is associated with hydrothermal breccia in the northeast corner of the map area (red dots; **Figure 6-2**). See the section **GEOLOGIC RESOURCES** for additional information on the breccias.

6.3 Fold structure in the Devine Ridge South 7.5' quadrangle

The rocks in the map area are locally folded. **Figure 6-2** and Plate 1 show two gently south-southwest plunging anticlines in the upper north-central and northeastern portions of the map area. An anticline is also present in the upper southeast part of the map area. The contact geometries and attitudes of these folds suggest the folding occurred after the 7 Ma Rattlesnake Tuff (**Tmtr**) was emplaced. Axes of the folds are cut by faults. The small anticlinal fold in the upper southeast part of the map area is interpreted as a drag fold within the Soldier Creek fault zone.

Figure 6-1. Evidence of faulting in the Devine Canyon Ash-flow Tuff (Tmdt) exposed along Forest Road 507 in the northeast corner of the study area disrupted by a small-offset (< 20 cm [8 in]), down-on-the-south normal fault (dashed line) (43.742654, -118.898515 WGS84 geographic coordinates; 4845042mE, 347131mN WGS84 UTM Zone 11 coordinates). Location number: 114 DRSCN 17; Scale bar 1 m (3.3 ft) high; hammer (arrow) 41 cm (16 in) length.

Figure 6-2. Structure map of the Devine Ridge South 7.5′ quadrangle, showing the distribution of faults (black lines) and folds (magenta lines). Base map is a 10-m slope shade displayed with 50 percent transparency; gray lines = roads.

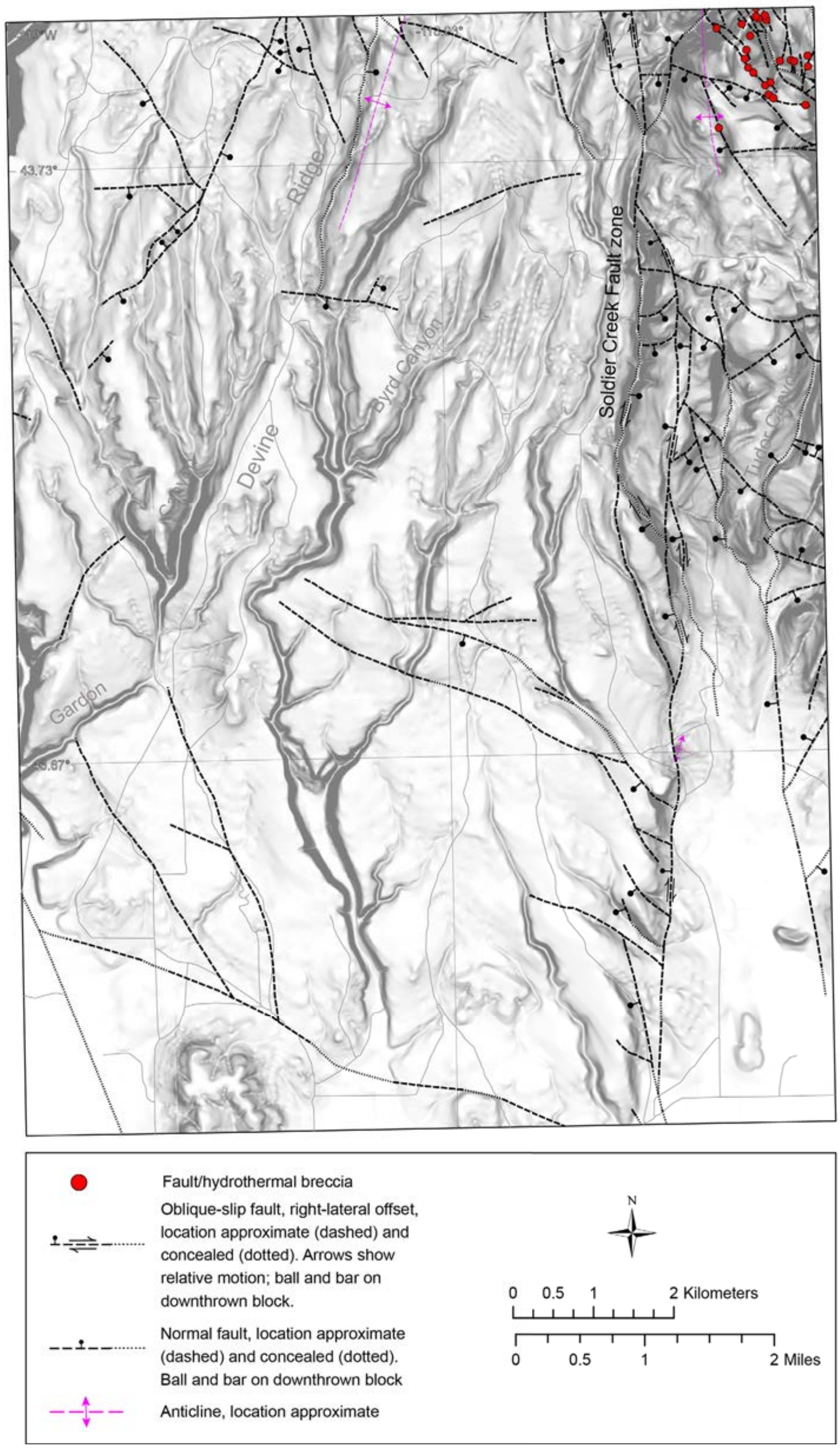

7.0 GEOLOGIC HISTORY

The nature of the "basement" rocks in the area is not known but can be assumed to be a series of Triassic/Jurassic flyschoid sedimentary rocks typical of the Izee Terrane (Wallace and Calkins, 1956). The basement is overlain/intruded by a locally erupted late Oligocene sequence of dacites, rhyolites, and andesites. This sequence is the first of three distinct eruptive episodes, along with later sedimentation, that span late Oligocene to late Pleistocene time. The following is the local geologic history pertaining to the Devine Ridge South 7.5′ quadrangle.

7.1 Idol City sequence

The sequence of eruptive and intrusive events in the late Oligocene, from oldest to youngest, is dacite (**Toda**), rhyolite (**Tor**), and andesite (**Toa**). These rocks, referred to here as the Idol City volcanics, are exposed in the highlands in the northern part of the map area. They are likely equivalent to those that form the mineralized host rock at the Idol City District in the Devine Ridge North 7.5′ quadrangle on the north. Rhyolitic dikes and irregular bodies (**Tor**) intrude the dacite in the northeast part of the quadrangle. The dacite (**Toda**) and rhyolite (**Tor**) rocks are associated with hydrothermal alteration features of epithermal gold deposits in the Idol City District.

7.2 Columbia River Basalt and Dinner Creek Tuff

In the map area a second albeit short-lived regional pulse of extrusive rocks, a basalt (**Tmb**) and 16 Ma Dinner Creek Tuff (**Tmdc**), produced a conspicuously thin sequence (M. L. Ferns, 2018, written commun.). These rocks are exposed in the highlands deposited on a pre-existing paleo-surface due to a combination of faulting and erosion. The basalts in adjacent quadrangles display similarities to Grand Ronde Basalt, Steens Basalt, and Picture Gorge Basalt (R. A. Houston and others, unpub. data, 2016; R. A. Houston and others, unpub. data, 2017) and suggest a composite succession of chemically distinct lavas. The basalt (**Tmb**) in the study area is apparently overlain by the 16 Ma Dinner Creek Tuff (**Tmdc**).

7.3 Devine Ash-flow Tuff, Prater Creek Ash-flow Tuff, and Rattlesnake Tuff

It is noteworthy that the study area contains a succession of three large ash-flow tuffs: 9.63 Ma Devine Canyon Ash-flow Tuff (**Tmtd**), 8.46 Ma Prater Creek Ash-flow Tuff (**Tmtp**), and 7.05 Ma Rattlesnake Tuff (**Tmtr**) (**Figure 5-1**; Plate 1). Emplacement of the Devine Canyon Ash-flow Tuff (**Tmtd**) and Prater Creek Ash-flow Tuff (**Tmtp**) temporarily interrupted the deposition of tuffaceous sedimentary rocks (unit **Tmst**). This unit appears to be deposited in a predominately fluvial environment. The Rattlesnake Tuff (**Tmtr**) conformably overlies the tuffaceous sedimentary rocks (**Tmst**) and is the youngest bedrock in the study area.

Of the three tuffs, the 7.05 Ma Rattlesnake Tuff (**Tmtr**) is among the most far-traveled with a reconstructed dense rock equivalent volume of 280 km^3 (67 mi^3) (Streck and Grunder, 1995). Caldera sources related to all three tuffs are not exposed locally but are thought to occur to the south in the Harney Basin (Walker, 1969; Walker, 1970; Greene, 1973; Parker, 1974; Walker, 1979; Streck and Grunder, 1995; Khatiwada and Keller, 2015). The map pattern of the three ash-flow tuffs forms a progressive offlapping sequence that becomes younger to the south and thickens outward into the Harney Basin (M. L. Ferns, 2018, written commun.).

7.4 Sedimentation

In the south part of the study area, patches of sedimentary rocks (**QTst**) cap the surface of the Rattlesnake Tuff (**Tmtr**). Source areas of the **QTst** strata were probably local from the ash-flow tuffs.

8.0 GEOLOGIC RESOURCES

8.1 Aggregate materials and industrial minerals

Summarized below in **Table 8-1** are the mineral resources in the Devine Ridge South 7.5′ quadrangle. Each type of commodity was rated based on the criteria explained by Goudarzi (1984). The list is limited to observed resources. Six historical sand and gravel sites were mined, all in the southern part of quadrangle (Niewendorp and Geitgey, 2009). These sand and gravel deposits are associated with Quaternary-Tertiary sedimentary rocks (**QTst**). The deposits constitute the known mineral occurrences in the quadrangle. However, without detailed geochemical sampling and a geophysics program, undiscovered precious metals and geothermal resources cannot be ruled out. Also, there is building stone potential for ash-flow tuff material, especially the crystal-poor Prater Creek Ash-flow Tuff (**Tmpt**). The reader is directed to Niewendorp and Geitgey (2009; https://www.oregongeology.org/milo/) for more information on the regional locations of aggregate and other mineral resources.

Table 8-1. Mineral resources observed in the Devine Ridge South 7.5′ quadrangle.

Type of Commodity	Resource Potential	Level of Certainty
Sand and gravel (borrow/fill/topsoil)	high*	high‡
Construction material (crushed/block)	no	
Limestone	no	
Clay	no	
Pumice	no	
Silica sand	no	
Bentonite	no	
Metals (precious, base)	no	
Coal	no	
Uranium and thorium	no	
Geothermal	no	
Oil and gas	no	
Other industrial minerals: gemstone materials, perlite, zeolite, manganese, titanium, zirconium	no	

*Abandoned mine land indicates the presence of resource (**QTst**).

‡Available information determined and/or confirmed that a surface mineral resource exists or there is the potential for one.

Located in the northeastern part of map area is hydrothermally altered and brecciated rock (**Figure 6-2**; **Figure 8-1**). These rocks have a lithologic association with the Idol City District, an epithermal gold deposit, where McGrane (1985) found similar rocks. Although additional mapping and analytical data are required to understand the spatial and temporal zoning of the hydrothermal alteration and brecciation, several field observations are worth mentioning:

- The primary host rocks for hydrothermal alteration and brecciation are dacites, but alteration is associated with younger(?) andesite and rhyolitic bodies/dikes as well (Plate 1).
- McGrane (1985) reported ages of 21.0 ± 0.9 Ma (K/Ar) on sericite alteration and 19.0 ± 0.08 Ma (K/Ar) on a rhyolite dike. However, an age on an andesite flow in the Idol City District (R. A. Houston, unpub. data, 2017) may further constrain the mineralizing event. In the map area

the altered and mineralized rocks are overlain by nonmineralized fresh basalt, indicating a chronological constraint on the timing of hydrothermal alteration and brecciation.

- The degree of alteration varies, but alteration is the most intense along breccia zones (tourmaline breccias, stockwork breccias, and rubble breccias; McGrane [1985]). McGrane (1985) identified four types of alteration in the Idol City District: tourmalinitic, sericitic, argillic, and propylitic, which were also recognized locally in the hydrothermal breccias.
- Visible precious or base metals were not observed in the hydrothermal breccias within the map area.
- There are no signs of exploration activity such as prospect pits, trenches, shafts, or adits within the alteration zones in the map area. Younger post-ore units cover the area and may conceal mineralization. Stream sediment and soil sampling might reveal zonation that extends under younger cover. A high-resolution gravity and magnetic survey would be informative.

Figure 8-1. A roughly tabular zone of hydrothermal brecciation and alteration rocks measuring about 50 m (164 ft) long and half as wide, elongated south to north. Shear zone with minor offset (dashed line), hoodoo (arrow). (43.749070, -118.882532 WGS84 geographic coordinates; 4845725mE, 348434mN WGS84 UTM Zone 11 coordinates). Location number 63 DRSCN 17; Scale bar 1 m (3.3 ft) tall.

8.2 Energy resources

The Devine Ridge South 7.5′ quadrangle has no potential for mineral fuel resources: coal, uranium, and thorium. Geothermal resources are not currently exploited in the map area and to the knowledge of the authors, no geothermal exploration has occurred in the mapped area, nor are there surface manifestations of past geothermal waters, such as deposits of siliceous sinter (https://www.oregongeology.org/gtilo/). There are some wells in the Harney 7.5′ quadrangle to the east with elevated water temperatures (Niewendorp and others, 2012).

No oil and gas exploration wells have been drilled in the Devine Ridge South 7.5′ quadrangle. However, during the late 1940s into the middle 1950s and then again in the late 1970s, the central and western regions of the Harney Basin were explored for oil and gas. Oil and gas well locations and drilling logs are available at https://www.oregongeology.org/mlrr/oilgas-logs.htm. Many of the wells reported shows of gas. A show is the appearance of oil and/or gas in cuttings, samples, or cores from drilling a well. Drilling records indicate that these wells were plugged and abandoned shortly after completion. This suggests that not all elements of a petroleum system for production of oil and/or gas are associated with the rocks within the Harney Basin, e.g., (1) a source rock for petroleum; (2) migration path(s); (3) reservoir rock; (4) seal; (5) trap; and (6) the geologic processes that form these elements. Therefore, the oil and gas potential of the Devine Ridge South 7.5′ quadrangle is none.

8.3 Water resources

A full discussion of the geologic controls on surface and groundwater resources in the Devine Ridge South 7.5′ quadrangle is beyond the scope of this report. The reader is referred to previous hydrogeologic investigations conducted by Piper and others (1939), Leonard (1970), Walker (1979), Whitehead (1994), and Gonthier (1985).

Water well data do accompany the geodatabase for this report. A well report query of Oregon Water Resources Department (OWRD) records for wells within the map area returned 31 wells (https://apps.wrd.state.or.us/apps/gw/well_log/). There are probably more wells in the map area than OWRD's records indicate. The wells are used for numerous purposes: domestic use, irrigation, and livestock. These wells cluster in the agricultural lowlands associated with the three main drainage areas in the map area: Poison Creek, Prater Creek, and Soldier Creek (Plate 1). The deepest well (HARN-134) was drilled to a depth of 221 m (725 ft) into "cinders"; its location is near the southeast corner of the map area. If cinders means either basalt or andesite, then mafic rocks (**Tmb**?, **Toa**?, and **Toda**?) underlie the ash-flow tuffs at this location and extend beyond the southern boundary of the study area.

9.0 GEOLOGIC HAZARDS

9.1 Landslide hazards

During this study, 16 landslide deposits in the form of simple and/or colluvial slides, rock fall, and debris flows were recognized and mapped in the Devine Ridge South 7.5′ quadrangle. Combined, these deposits cover 0.005 percent of the map area, which is 72.66 hectares (179.55 acres). More landslides smaller than 100 m^2 (1,075 ft^2) may be present in the study area. Small slides are difficult to recognize because of the resolution of the SFM DEM. Improvements in surface imagery, such as acquisition of high-resolution lidar, would result in the identification of more landslides with greater accuracy and confidence.

Field checking of landslides was very limited. Thus, Plate 1 cannot serve as a substitute for site-specific studies in critical areas. The downslope movement of rock and soil, in the form of landslides, rock falls, and debris flows may present a geologic hazard to residents, infrastructure, and transportation corridors in the Devine Ridge South 7.5′ quadrangle. Three general types of landslide processes present in the map area, including slides (simple and colluvial), rock fall, and debris-flows, are described in more detail below.

9.1.1 Slides

A typical slide in the Devine Ridge South study area covers less than 5.46 hectares (13.5 acres), while the largest is over 31 hectares (76.6 acres). Unfortunately, due to the limitations of our study, we did not investigate each slide to categorize movement or behavior based on Varnes (1978) and USGS (Highland, 2004) methodologies.

Slides can be attributed to the combined influences of parallel topographic slope and bedding dip, undercutting by streams, heavy precipitation, groundwater conditions, and rock type, e.g., moderate to steep slopes underlain by weakly consolidated tuffaceous sedimentary rocks (**Tmst**; Plate 1). Future landsliding should be expected in association with **Tmst**, particularly in areas of changing vegetation resulting from rangeland fires or changing land use that may alter local groundwater conditions.

Some slopes in the study area are mantled by unstable wedges of soil and rock. These deposits are not differentiated from landslides. Colluvial deposits typically form when weathered rock particles, ranging in size from clay to boulders, accumulate along a hillside. When the mass of the accumulated material reaches a critical size, a triggering event such as heavy rainfall or seismogenic event may initiate the rapid down slope movement of this mass. Areas denuded by fire or other anthropogenic vegetative removal can especially be at risk from such events.

9.1.2 Rock falls

Rock fall and rockslide hazards may be present in the study area where steep slopes and cliff exposures of **Toda**, **Tmtd**, **Tmtp**, and **Tmtr** occur (Plate 1). Potential natural triggering mechanisms for rock fall events include freeze/thaw conditions, heavy rainfall, earthquakes, and extensive devegetation due to fire.

9.1.3 Alluvial fan deposits

Alluvial fan and debris fan (**Qaf**) deposits in the study area have been mapped in the Prater Creek and tributaries of Poison Creek (Plate 1) drainages. Rapidly moving landslides in the form of debris flows may be expected on both alluvial and debris fans that lie at the mouths of steep-sided, colluvium-filled canyons and upland drainages. The potential for inundation of fan areas by rapidly moving debris flows increases during episodes of intense rainfall that occur after soils have been saturated by fall and early winter rainfall. Redirected drainage and poor construction practices are human activities that could initiate debris flows (Beaulieu, 1977). Debris flows have the potential to threaten life and may cause extensive damage to property and transportation corridors.

10.0 ACKNOWLEDGMENTS

This project and publication were supported through the STATEMAP component of the National Cooperative Geologic Mapping Program under cooperative agreement number G17AC00210. Additional funds were provided by the State of Oregon. XRF geochemical analyses were prepared and analyzed by Dr. Scott Buroughs at the GeoAnalytical Lab at Washington State University. The authors appreciate informative discussions and field trips with Ivan Gall, Justin Iverson, Jerry Grondin, Darrick Boschmann, and other geologists who provided their expertise on stratigraphy in the Harney Basin. The authors acknowledge several area landowners who provided local knowledge and graciously allowed access to private holdings within the study area. Cartography for the map plates was provided by John Franczyk. Critical and insightful reviews by Darrick Boschmann, Mark Ferns, and Jed Roberts greatly enriched the final manuscript, geodatabase, and geologic map.

11.0 REFERENCES

Baksi, A. K., 1989, Reevaluation of the timing and duration of extrusion of the Imnaha, Picture Gorge, and Grand Ronde Basalts, Columbia River Basalt Group, *in* Reidel, S.P., and Hooper, P.R., eds., Volcanism and tectonism in the Columbia River flood-basalt province: Boulder, Colo., Geological Society of America Special Paper 239, p. 105–112. https://doi.org/10.1130/SPE239-p105

Beaulieu, J. D., 1977, Geologic hazards of parts of northern Hood River, Wasco, and Sherman Counties, Oregon: Oregon Department of Geology and Mineral Industries Bulletin 91, 95 p. 11 pl., scale 1:62,500. https://www.oregongeology.org/pubs/B/B-091.pdf

Boschmann, D. E., 2012, Structural and volcanic evolution of the Glass Buttes area, High Lava Plains, Oregon: Corvallis, Oreg., Oregon State University, M.S. thesis, 100 p. https://ir.library.oregonstate.edu/concern/graduate_thesis_or_dissertations/47429d66f

Brown, C. E., and Thayer, T. P., 1966, Geologic map of the Canyon City quadrangle, northeastern Oregon: U.S. Geological Survey Miscellaneous Geologic Investigations Map I-447, 1 pl., scale 1:250,000.

Brown, D. E., 1982, Map showing geology and geothermal resources of the southern half of the Burns 15 minute quadrangle, Oregon: Oregon Department of Geology and Mineral Industries Geological Map Series GMS-20, 1 pl., scale 1:24,000. https://www.oregongeology.org/pubs/gms/GMS-020.pdf

Brown, D. E., McLean, G. D., and Black, G. L., 1980, Preliminary geology and geothermal resource potential of the northern Harney Basin, Oregon: Oregon Department of Geology and Mineral Industries Open-File Report 80-6, 52 p., 4 pl., scale 1:62,500. Zipped file: https://www.oregongeology.org/pubs/ofr/O-80-06.zip

Cahoon, E. B., and Streck, M. J., 2017, Picture gorge basalt, eastern Oregon: Extended distribution and petrogenetic connections to Steens basalt and Strawberry Volcanics: Geological Society of America Abstracts with Programs, v. 49, no. 6. doi: 10.1130/abs/2017AM-304582. https://gsa.confex.com/gsa/2017AM/webprogram/Paper304582.html

Camp, V. E., Ross, M. E., and Hanson, W. E., 2003, Genesis of flood basalts and Basin and Range volcanic rocks from Steens Mountain to the Malheur River Gorge, Oregon: Geological Society of America Bulletin, v. 115, no. 1, p. 105–128. https://doi.org/10.1130/0016-7606(2003)115<0105:GOFBAB>2.0.CO;2

Camp, V. E., Ross, M. E., Duncan, R. A., Jarboe, N. A., Coe, R. S., Hanan, B. B., and Johnson, J. A., 2013, The Steens Basalt: Earliest lavas of the Columbia River Basalt Group, *in* Reidel, S. P., Camp, V. E., Ross, M. E., Wolff, J. A., Martin, B. S., Tolan, T. L., and Wells, R. E., The Columbia River Flood Basalt Province: Geological Society of America Special Paper 497, p. 87–116. https://doi.org/10.1130/2013.2497(04)

Cohen, K. M., Finney, S. C., Gibbard, P. L., and Fan, J.-X., 2013, The ICS International Chronostratigraphic Chart: Episodes, v. 36, no. 3, 199–204. http://www.stratigraphy.org/ICSchart/Cohen2013_Episodes.pdf

Donath, F. A., 1962, Analysis of basin-range structure, south-central Oregon: Geological Society of America Bulletin, v. 73, p. 1–16. https://doi.org/10.1130/0016-7606(1962)73[1:AOBSSO]2.0.CO;2

Ferns, M. L., and McClaughry, J. D., 2013, Stratigraphy and volcanic evolution of the middle Miocene to Pliocene La Grande–Owyhee eruptive axis in eastern Oregon, *in* Reidel, S. P., Camp, V. E., Ross, M. E., Wolff, J. A., Martin, B. S., Tolan, T. L., and Wells, R. E., eds., The Columbia River Flood Basalt Province: Geological Society of America Special Paper 497, p. 401–427. https://doi.org/10.1130/2013.2497(16)

Ferns, M. L., Brooks, H. C., Evans, J. G., and Cummings, M. L., 1993, Geologic map of the Vale 30 × 60 minute quadrangle, Malheur County, Oregon, and Owyhee County, Idaho: Oregon Department of Geology and Mineral Industries Geologic Map Series GMS-77, 1 pl., scale 1:100,000. https://www.oregongeology.org/pubs/gms/GMS-077.pdf

Ford, M. T., Grunder, A. L., and Duncan, R. A., 2013, Bimodal volcanism of the High Lava Plains and northwestern Basin and Range of Oregon: Distribution and tectonic implications of age-progressive rhyolites: Geochemistry, Geophysics, Geosystems, v. 14, no. 8, p. 2837–2857. https://doi.org/10.1002/ggge.20175

Geological Society of America Rock-Color Chart Committee, 1991, Rock color chart, 7th printing: Boulder, Colo.

Gillespie, M. R., and Styles, M. T., 1999, BGS rock classification scheme, v. 1, Classification of igneous rocks: Keyworth, U.K., British Geological Survey Research Report RR 99-06 (reformatted), 52 p. http://nora.nerc.ac.uk/3223/1/RR99006.pdf

Gonthier, J. B., 1985, A description of aquifer units in eastern Oregon: U.S. Geological Survey Water-Resources Investigations Report 84-4095, 39 p., 4 pl., scale 1:500,000. https://doi.org/10.3133/wri844095

Gradstein, F. M., and others. 2004, A geologic time scale 2004: Cambridge University Press, 589 p.

Gray, J. J., Peterson, N. V., Clayton, J., and Baxter, G. L., 1983, Geology and mineral resources of 18 BLM Wilderness Study Areas, Harney and Malheur Counties, Oregon: Oregon Department of Geology and Mineral Industries Open-File Report O-83-2. https://www.oregongeology.org/pubs/ofr/O-83-02.pdf

Greene, R. C., 1972, Preliminary geologic map of the Burns and West Myrtle Butte 15-minute quadrangles, Oregon: U.S. Geological Survey Miscellaneous Field Studies Map MF-320, scale 1:62,500. https://ngmdb.usgs.gov/Prodesc/proddesc_2743.htm

Greene, R. C., 1973, Petrology of the welded tuff of Devine Canyon, southeast Oregon: U.S. Geological Survey Professional Paper 797, 26 p. https://doi.org/10.3133/pp797

Greene, R. C., Walker, G. W., and Corcoran, R. E., 1972, Geologic map of the Burns quadrangle, Oregon: U.S. Geological Survey Miscellaneous Geologic Investigations Map I-680, scale 1:250,000. https://ngmdb.usgs.gov/Prodesc/proddesc_9455.htm

Hallsworth, C. R., and Knox, R. W. O'B., 1999, BGS rock classification scheme, v. 3, Classification of sediments and sedimentary rocks: Keyworth, U.K., British Geological Survey Research Report RR 99-03, 44 p. http://nora.nerc.ac.uk/3227/1/RR99003.pdf

Highland, L. (compiler), 2004, Landslide types and processes: U.S. Geological Survey Fact Sheet 2004-3072, version 1.1. https://pubs.usgs.gov/fs/2004/3072/pdf/fs2004-3072.pdf

Isom, S. L., 2017, Compositional and physical gradients in the magmas of the Devine Canyon Tuff, eastern Oregon: constraints for evolution models of voluminous high-silica rhyolites: Portland, Oreg., Portland State University, M.S. thesis, 147 p. https://pdxscholar.library.pdx.edu/open_access_etds/3885/

Johnson, D. M., Hooper, P. R., and Conrey, R. M., 1999, XRF analysis of rocks and minerals for major and trace elements on a single low dilution Li-tetraborate fused bead: Advances in X-ray Analysis, v. 41, p. 843–867. https://s3.wp.wsu.edu/uploads/sites/2191/2017/06/Johnson-Hooper-and-Conrey.pdf

Johnson, J. A., 1994, Geologic map of the Krumbo Reservoir quadrangle, Harney County, southeastern Oregon: U.S. Geological Survey Miscellaneous Field Studies Map MF-2267, 11 p., 1 pl., scale 1:24,000. https://pubs.er.usgs.gov/publication/mf2267

Johnson, J. A., 1996, Geologic map of the Page Springs quadrangle, Harney County, southeastern Oregon: U.S. Geological Survey Open-File Report OF-96-675, 1 pl., scale 1:24,000. https://ngmdb.usgs.gov/Prodesc/proddesc_18672.htm

Johnson, J.A., Hooper, P.R., Hawkesworth, C. J., and Binger, G. B., 1998, Geologic map of the Stemler Ridge quadrangle, Malheur County, southeastern Oregon: U.S. Geological Survey Open-File Report OF-98-105, 1 pl., scale 1:24,000. https://ngmdb.usgs.gov/Prodesc/proddesc_16445.htm

Jordan, B. T., Streck, M. J., and Grunder, A. L., 2002, Bimodal volcanism and tectonism of the High Lava Plains, Oregon, *in* Moore, G. W., ed., Field guide to geologic processes in Cascadia, Field trips to accompany the 98th Annual Meeting of the Cordilleran Section of the Geological Society of America, May 13–15, 2002, Corvallis, Oregon: Oregon Department of Geology and Mineral Industries Special Paper 36, p. 23–46. https://www.oregongeology.org/pubs/sp/SP-36.pdf

Jordan, B. T., Grunder, A. L., Duncan, R. A., and Deino, A. L., 2004, Geochronology of age-progressive volcanism of the Oregon High Lava Plains: Implications for the plume interpretation of Yellowstone: Journal of Geophysical Research, v. 109, no. B10, B10202, 19 p. https://doi.org/10.1029/2003JB002776

Khatiwada, M., and Keller, G. R., 2015, An integrated geophysical imaging of the upper crustal features in the Harney Basin, southeast Oregon: Geosphere, v. 11, no. 1, p. 185–200. https://doi.org/10.1130/GES01046.1

Kittleman, L. R., Green, A. R., Hagood, A. R., Johnson, A. M., McMurray, J. M., Russell, R. G., and Weeden, D. A., 1965, Cenozoic stratigraphy of the Owyhee region, southeastern Oregon: University of Oregon, Museum of Natural History Bulletin, no. 1, 45 p. https://scholarsbank.uoregon.edu/xmlui/handle/1794/19996

Lawrence, R. D., 1976, Strike-slip faulting terminates the Basin and Range province in Oregon: Geological Society of America Bulletin, v. 87, no. 6, p. 846–850. https://doi.org/10.1130/0016-7606(1976)87<846:SFTTBA>2.0.CO;2

Le Bas, M. J., and Streckeisen, A. L., 1991, The IUGS systematics of igneous rocks: Journal of the Geological Society, v. 148, no. 5, p. 825–833. https://doi.org/10.1144/gsjgs.148.5.0825

Le Bas, M. J., Le Maitre, R. W., Streckeisen, A., and Zanettin, B., 1986, A chemical classification of volcanic rocks based on the total alkali-silica diagram: Journal of Petrology, v. 27, no. 3, p. 745–750. https://doi.org/10.1093/petrology/27.3.745

Le Maitre, R. W., and others, 1989, A classification of igneous rocks and glossary of terms: Recommendations of the International Union of Geological Sciences Subcommission on the Systematics of Igneous Rocks: Oxford, Blackwell, 193 p.

Le Maitre, R. W. (ed.), and others, 2004, Igneous rocks: a classification and glossary of terms: recommendations of the International Union of Geological Sciences, Subcommission on the Systematics of Igneous Rocks: Cambridge, Cambridge University Press, 236 p.

Leonard, A. R., 1970, Ground-water resources in Harney Valley, Harney County, Oregon: Salem, Oreg., Oregon Water Resources Department, Ground Water Report 16, 65 p., 3 pl., scale 1:125,000. https://www.oregon.gov/owrd/wrdreports/gw_report_16_harney.pdf

Mackenzie, W. S., Donaldson, C. H., and Guilford, C., 1997, Atlas of igneous rocks and their textures (7th ed.): Addison Wesley Longman, 148 p.

MacLeod, N. S., Walker, G. W., and McKee, E. H., 1976, Geothermal significance of eastward increase in age of upper Cenozoic rhyolitic domes in southeastern Oregon, *in* Second United Nations Symposium on the Development and Use of Geothermal Resources, v. 1: Washington D.C., Government Printing Office, p. 465–474.

McGrane, D, J., 1985, Geology of the Idol City area: a volcanic-hosted, disseminated precious-metal occurrence in east-central Oregon: Missoula, Mont., University of Montana, M.S. thesis, 88 p. https://scholarworks.umt.edu/etd/7536

Meigs, A., and others, 2009, Geological and geophysical perspectives on the magmatic and tectonic development, High Lava Plains and northwest Basin and Range, *in* O'Connor, J. E., Dorsey, R. J., and Madin, I. P., GSA Field Guide 15, Volcanoes to Vineyards: Boulder, Colo., Geological Society of America. https://doi.org/10.1130/2009.fld015(21)

Milliard, J. B., 2010, Two-stage opening of the northwestern Basin and Range in eastern Oregon: Evidence from the Miocene Crane Bbasin: Corvallis, Oreg., Oregon State University, M.S. thesis, 82 p.

Minor, S. A., Rytuba, J. J., Grubensky, M. J., Meulen, D. B. V., Goeldner, C. A., and Tegtmeyer, K. J., 1987a, Geologic map of the High Steens and Little Blitzen Gorge Wilderness Study areas, Harney County, Oregon: U.S. Geological Survey Miscellaneous Field Studies Map MF-1876, 1 pl., scale 1:24,000. https://ngmdb.usgs.gov/Prodesc/proddesc_7460.htm

Minor, S. A., Rytuba, J. J., Vander Meulen, D. B., Grubensky, M. J., and Tegtmeyer, K. J., 1987b, Geologic map of the Wildhorse Lake quadrangle, Harney County, Oregon: U.S. Geological Survey Miscellaneous Field Studies Map MF-1915, 1 pl., scale 1:24,000. https://ngmdb.usgs.gov/Prodesc/proddesc_5480.htm

NCGMP (USGS National Cooperative Geologic Mapping Program), 2010, NCGMP09—Draft standard format for digital publication of geologic maps, version 1.1, *in* Soller, D. R., ed., Digital Mapping Techniques '09—Workshop Proceedings: U.S. Geological Survey Open-File Report 2010–1335, p. 93–146. https://pubs.usgs.gov/of/2010/1335/pdf/usgs_of2010-1335.pdf

Niem, A. R., 1974, Wright's Point, Harney County, Oregon: an example of inverted topography: Ore Bin, v. 36, no. 3, 33–49. https://www.oregongeology.org/pubs/OG/OBv36n03.pdf

Niewendorp, C. A., and Geitgey, R. P., 2009, Mineral information layer for Oregon (MILO), release 2, GIS files. https://www.oregongeology.org/milo/index.htm

Niewendorp, C. A., Ricker, T. R., Rabjohns, K. W., and Brodie, S. H., 2012, Geothermal information layer for Oregon (GTILO), release 2, GIS files. https://www.oregongeology.org/gtilo/index.htm

Ogg, J. G., Ogg, G., and Gradstein, F. M., 2008, The concise geologic time scale: Cambridge University Press, 184 p.

Orr, E. L., Orr, W. N., and Baldwin, E. M., 1992, Geology of Oregon, 4th ed.: Dubuque, Iowa, Kendall/Hunt Publishing Company, 254 p.

Parker, D. J., 1974, Petrology of selected volcanic rocks of the Harney Basin, Oregon: Corvallis, Oreg., Oregon State University, Ph.D. dissertation, 153 p., 1 pl. https://ir.library.oregonstate.edu/concern/graduate_thesis_or_dissertations/r494vn606

Piper, A. M., Robinson, T. W., and Park C. F., 1939, Geology and ground-water resources of the Harney Basin, Oregon: U.S. Geological Survey Water Supply Paper 841, 189 p., 1 pl., scale 1:125,000. https://pubs.er.usgs.gov/publication/wsp841

Reidel, S. P., Johnson, V. G., and Spane, F. A., 2002, Natural gas storage in basalt aquifers of the Columbia Basin, Pacific Northwest USA: A guide to site characterization: Richland, Wash., Pacific Northwest Laboratory PNNL-13962. https://www.pnnl.gov/main/publications/external/technical_reports/PNNL-13962.pdf

Robertson, S., 1999, BGS rock classification scheme, v. 2, Classification of metamorphic rocks: Keyworth, U.K., British Geological Survey Research Report RR 99-02, 24 p. http://nora.nerc.ac.uk/id/eprint/3226/1/RR99002.pdf

Russell, I. C., 1884, A geological reconnaissance in southern Oregon: U.S. Geological Survey Annual Report 4 (1882-1883), p. 431–464. https://doi.org/10.3133/ar4

Scarberry, K., Grunder, A., and Meigs, A., 2007, Transition from intermediate to bimodal volcanism and inception and style of extensional faulting within the margin of the basin and range province, southern Oregon: Eos, Trans AGU, v. 88.

Sheppard, R. A., and Gude, A. J., III, 1993, Geology and mineralogy of the Harney Lake zeolite deposit, Harney County, Oregon, *in* Ming, D. W., and Mumpton, F. A., eds., Zeo-Trip '93: An excursion to selected zeolite and clay deposits in southeastern Oregon and southwestern Idaho, June 26–28, 1993: Brockport, N.Y., International Committee on Natural Zeolites, p. 42–58.

Sherrod, D. R., and Johnson, J. A., 1994, Geologic map of the Irish Lake quadrangle, Harney County, south-central Oregon: U.S. Geological Survey Miscellaneous Field Studies Map MF-2256, 1 sheet, scale 1:24,000. https://ngmdb.usgs.gov/Prodesc/proddesc_5877.htm

Smith, G. A., 1986a, Stratigraphy, sedimentology, and petrology of Neogene rocks in the Deschutes Basin, central Oregon: a record of continental margin volcanism and its influence on fluvial sedimentation in an arc-adjacent basin: Corvallis, Oreg., Oregon State University, Ph.D. dissertation, 467 p, 3 pl., scale 1:24,000.

Smith, G. A., 1986b, Stratigraphy, sedimentology, and the petrology of Neogene rocks in the Deschutes Basin, central Oregon: A record of continental-margin volcanism and its influence on fluvial sedimentation in an arc-adjacent basin: Richland, Wash., U.S. Department of Energy Basalt Waste Isolation Project, Rockwell Hanford Operations Publication RHO-BW-SA-555 P, 1 pl., scale 1:24,000.

Smith, J. V., and MacKenzie, W. S., 1958, The cooling history of high-temperature sodium-rich feldspars, pt. 4 *of* The alkali feldspars: Am. Mineralogist, v. 43, no. 9-10, p. 872–889.

Smith, R. L., and Roe, W. P., 2015, Oregon geologic data compilation [OGDC], release 6 (statewide): Oregon Department of Geology and Mineral Industries Digital Data Series OGDC-6, geodatabase. https://www.oregongeology.org/pubs/dds/p-OGDC-6.htm

Streck, M. J., 1994, Volcanology and petrology of the Rattlesnake Ash-Flow Tuff, eastern Oregon: Corvallis, Oreg., Oregon State University, Ph.D. dissertation, 184 p.

Streck, M., and Ferns, M., 2004, The Rattlesnake Tuff and other Miocene silicic volcanism in eastern Oregon, chap. 1 *of* Haller, K. M., and Wood, S. H., Geological field trips in southern Idaho, eastern Oregon, and northern Nevada: U.S. Geological Survey Open-File Report 2004-1222, p. 4–19. https://pubs.usgs.gov/of/2004/1222/

Streck, M. J., and Grunder, A. L., 1995, Crystallization and welding variations in a widespread ignimbrite sheet; the Rattlesnake Tuff, eastern Oregon, USA: Bulletin of Volcanology, v. 57, no. 3, p. 151–169. https://doi.org/10.1007/BF00265035

Streck, M. J., Johnson, J. A., and Grunder, A. L., 1999, Field guide to the Rattlesnake Tuff and High Lava Plains near Burns, Oregon: Ore Bin, v. 61, no. 3, 64-76. https://www.oregongeology.org/pubs/og/OGv61n03.pdf

Streck, M. J., Ferns, M. L., and McIntosh, W., 2015, Large, persistent rhyolitic magma reservoirs above Columbia River Basalt storage sites: The Dinner Creek Tuff Eruptive Center, eastern Oregon: Geological Society of America, Geosphere, v. 11, no. 2, 226–235. doi:10.1130/GES01086.1

Thompson, G. A., and Burke, D. B., 1974, Regional geophysics of the Basin and Range province: Ann. Rev. Earth Planet. Sci., v. 2, 213-238. https://doi.org/10.1146/annurev.ea.02.050174.001241

Thormahlen, D. J., 1984, Geology of the northwest one-quarter of the Prineville quadrangle, central Oregon: Corvallis, Oreg., Oregon State University, M.S. thesis, 106 p. 1 pl., scale 1:24,000.

Trench, D., 2008, The termination of the Basin and Range Province into a clockwise rotating region of transtension and volcanism, central Oregon: Corvallis, Oreg., Oregon State University, M.S. thesis, 64 p.

Varnes, D. J., 1978, Slope movement types and processes, Chap. 2 *in* Schuster, R. L., and Krizek, R. J., eds., Landslides: analysis and control: Washington D. C., National Academy Press, Transportation and Road Research Board Special Report 176, p. 11–33.

Walker, G. W., 1969, Geology of the High Lava Plains Province, *in* Weissenborn, A. W., ed., Mineral and water resources of Oregon: Oregon Department of Geology and Mineral Industries Bulletin 64, p. 77–79. https://www.oregongeology.org/pubs/B/B-064.pdf

Walker, G. W., 1970, Cenozoic ash-flow tuffs of Oregon: Ore Bin, v. 32, no. 6, 97–115. https://www.oregongeology.org/pubs/OG/OBv32n06.pdf

Walker, G. W., 1977, Geologic map of Oregon east of the 121st meridian: U.S. Geological Survey Miscellaneous Investigations Map I-902, 2 sheets, scale 1:500,000. https://ngmdb.usgs.gov/Prodesc/proddesc_9795.htm

Walker, G. W., 1979, Revisions to the Cenozoic stratigraphy of Harney Basin, southeastern Oregon: U.S. Geological Survey Bulletin 1475, 35 p., 1 pl. https://doi.org/10.3133/b1475

Walker, G. W., and MacLeod, N. S., 1991, Geologic map of Oregon: U.S. Geological Survey, scale 1:500,000. https://ngmdb.usgs.gov/Prodesc/proddesc_16259.htm

Walker, G. W., and Repenning, C. A., 1965, Reconnaissance geologic map of the Adel quadrangle, Lake, Harney, and Malheur Counties, Oregon: U.S. Geological Survey, Miscellaneous Geologic Investigations Map IMAP-446, 1 pl., scale 1:250,000. https://doi.org/10.3133/i446

Wallace, R. E., and Calkins, J. A., 1956, Reconnaissance geologic map of the Izee and Logdell quadrangles, Oregon: U.S. Geological Survey Miscellaneous Field Studies Map MF-82, scale 1:62,500. https://ngmdb.usgs.gov/Prodesc/proddesc_2988.htm

Wentworth, C. K., 1922, A scale of grade and class terms of clastic sediments: Journal of Geology, v. 30, no. 5, p. 377–392.

Whitehead, R. L., 1994, Ground water atlas of the United States: Segment 7, Idaho, Oregon, Washington: U.S. Geological Survey Hydrologic Atlas 730-H, 31 p. https://doi.org/10.3133/ha730H

12.0 APPENDIX

This appendix contains a summary of the geodatabase along with a description of analytical and field methods and the list of attribute fields for spreadsheets (see page 7 of this report). The appendix is divided into two sections:

- Section 12.1 describes the digital databases included with this publication.
- Section 12.2 contains a summary of analytical and field methods. Accompanying tables explain the fields listed in various spreadsheets.

12.1 Geographic information systems (GIS) database

Geodatabase specifications

Digital data created for the Devine Ridge South 7.5′ quadrangle are stored in an Esri format geodatabase. The geodatabase structure follows that outlined by the U.S. Geological Survey (USGS) National Cooperative Geologic Mapping Program 2009 draft standard format for digital publication of geologic maps, version 1.1 (NCGMP, 2010). The following information describes the overall database structure, the feature classes, and supplemental tables (**Figure 12-1**, **Figure 12-2**, **Figure 12-3**, **Table 12-1**, and **Table 12-2**).

The data are stored in a file geodatabase feature dataset (GeologicMap). Accessory file geodatabase tables (DataSources, DescriptionOfMapUnits, Glossary) were created by using ArcGIS version 10.2.2 (SP 1). The GeologicMap feature dataset contains all the spatially oriented data (feature classes) created for the Devine Ridge South 7.5′ quadrangle. The file geodatabase tables are used to hold additional geologic attributes.

Figure 12-1. Devine Ridge South 7.5′ quadrangle geodatabase feature dataset and data tables.

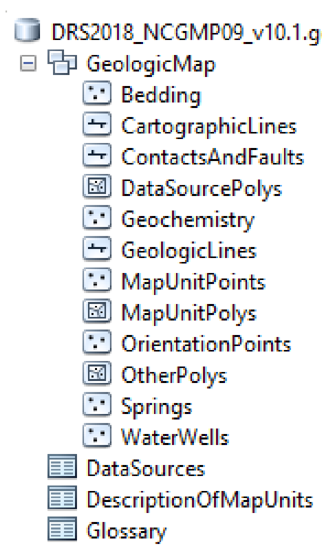

Geodatabase feature class specifications

Each feature class within the GeologicMap feature dataset in the geodatabase contains detailed metadata. Please see the metadata for detailed information such as process descriptions, accuracy specifications, and entity attribute descriptions.

Figure 12-2. Devine Ridge South 7.5' quadrangle geodatabase feature classes and descriptions.

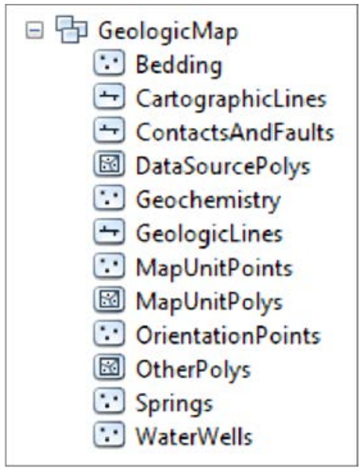

Table 12-1. Feature class description.

Name	Description
Bedding	This feature class represents point locations in the quadrangle where bedding measurements were made or were compiled from previous studies. These data are also contained in the bedding (strike and dip) spreadsheet described in more detail below.
CartographicLines	Vector lines that have no real-world physical existence and do not participate in map-unit topology. The feature class includes cross section lines used for cartography for the quadrangle.
ContactsAndFaults	The vector lines in this feature class contains geologic content including contacts and fault locations used to create the map unit polygon boundaries. The existence and location confidence values for the contacts and faults are provided in the feature class attribute table.
DataSourcePolys	This feature class contains polygons that delineate data sources for all parts of the geologic map. These sources may be a previously published map, new mapping, or mapping with a certain technique. For a map with one data source, for example all new mapping, this feature class contains one polygon that encompasses the map area.
Geochemistry	This feature class represents point locations where whole-rock samples have been analyzed by X-ray fluorescence (XRF) techniques in the quadrangle. Includes data collected by the authors during this study or compiled from previous studies. These data are also contained in the geochemistry spreadsheet described in more detail below.
GeologicLines	These vector lines represent known fold axis locations in the quadrangle. The existence and location confidence for the fold axes are provided in the feature class attribute table.
MapUnitPoints	This feature class represents points used to generate the MapUnitPolys feature class from the ContactsAndFaults feature class.
MapUnitPolys	This polygon feature class represents the geologic map units as defined by the authors.
OrientationPoints	This feature class represents point locations in the quadrangle where bedding measurements were made or were compiled from previous studies. These data are also contained in the bedding (strike and dip) spreadsheet described in more detail below.
OtherPolys	This feature class depicts the reference map for the quadrangle study area.
Springs	This feature class represents point locations where springs were in the quadrangle. Includes data observed or inferred by the authors or obtained by the authors from the Pacific Northwest Hydrography Framework (PNWHF). These data are also contained in the Springs spreadsheet.
WaterWells	This feature class represents point locations of water wells in the quadrangle. Includes data obtained by the authors from the Oregon Department of Water Resources (OWRD). These data are also contained in the WaterWell spreadsheet described in more detail below.

Geodatabase table specifications

Figure 12-3. Devine Ridge South 7.5′ quadrangle geodatabase data tables.

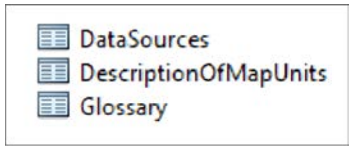

Table name description

Table 12-2. Accompanying tables.

Name	Description
DataSources	Data table that contains information about data sources used to compile the geology of the area.
DescriptionOfMapUnits	Data table that captures the content of the Description of Map Units (DMU), or equivalent List of Map Units and associated pamphlet text, included in a geologic map.
Glossary	Data table that contains information about the definitions of terms used in the geodatabase.

Geodatabase projection specifications

All spatial data are stored in the Oregon Statewide Lambert Conformal Conic projection. The datum is NAD83 HARN. The linear unit is international feet. See detailed projection parameters below:

Projection: Lambert_Conformal_Conic
False_Easting: 1312335.958005
False_Northing: 0.000000
Central_Meridian: -120.500000
Standard_Parallel_1: 43.000000
Standard_Parallel_2: 45.500000
Latitude_Of_Origin: 41.750000
Linear Unit: Foot (0.304800)

Geographic Coordinate System: GCS_North_American_1983_HARN
Angular Unit: Degree (0.0174532925199433299)
Prime Meridian: Greenwich (0.000000000000000000)
Datum: D_North_American_1983_HARN
Spheroid: GRS_1980
Semimajor Axis: 6378137.000000000000000000
Semiminor Axis: 6356752.314140356100000000
Inverse Flattening: 298.257222101000020000

Geologic map

This report is accompanied by a map plate displaying the surficial and bedrock geology at a scale of 1:24,000 and a geologic cross section (Plate 1 facsimile below) for the Devine Ridge South 7.5′ quadrangle. The map plate was generated from detailed geologic data (scale of 1:8,000 or better) contained in the accompanying Esri format geodatabase. Both bedrock and surficial geologic interpretations can be recovered from the geodatabase and can be used to create a variety of additional thematic maps.

Plate 1. Geologic map of the Devine Ridge South 7.5′ quadrangle, Harney County, Oregon, Plate dimensions are 34 by 41 inches. See digital folder for map plate.

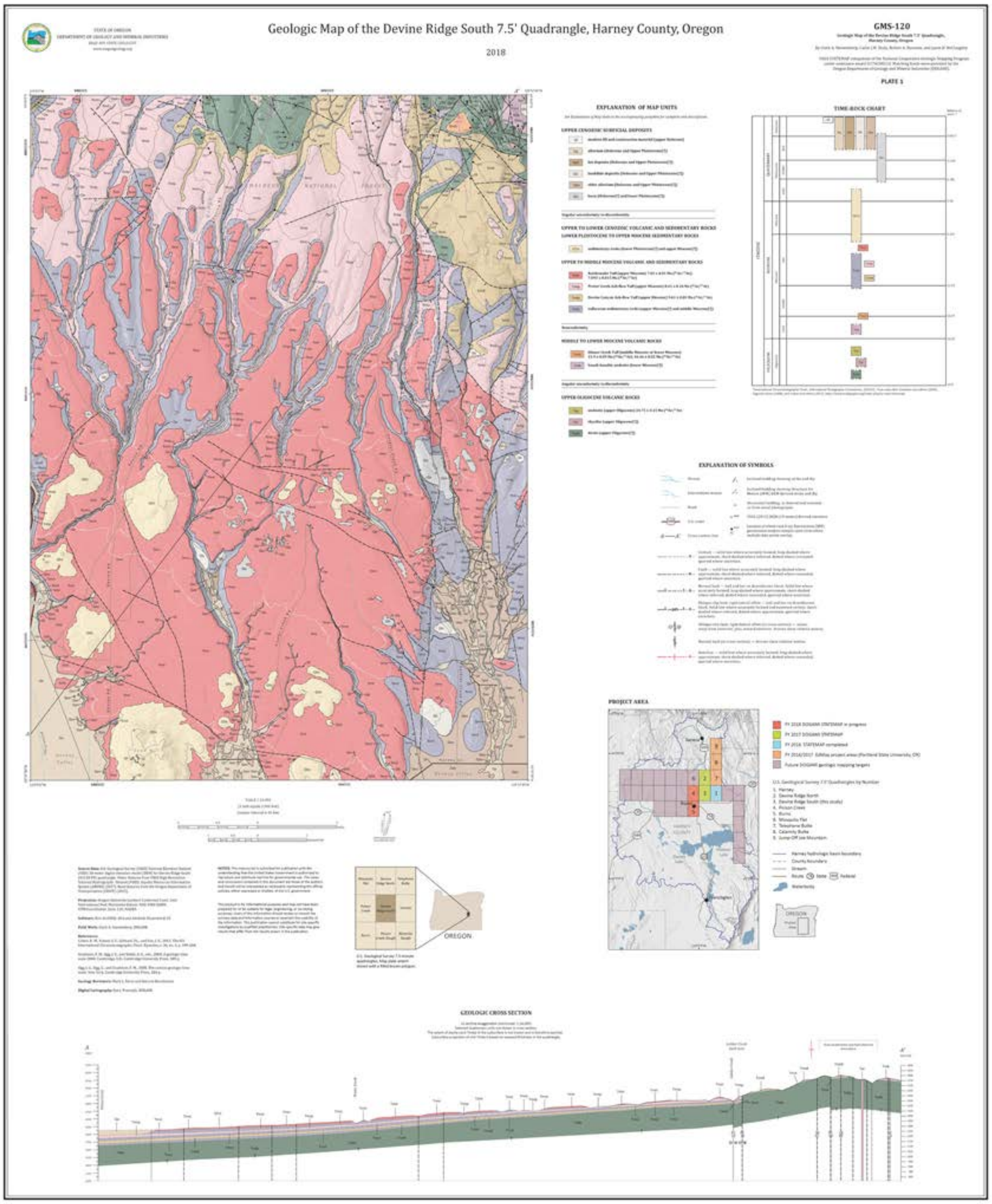

12.2 Methods

Geochemical analytical methods

Geologic mapping in the Devine Ridge South 7.5′ quadrangle was supported by numerous new and compiled X-ray fluorescence (XRF) geochemical analyses of whole-rock samples. Descriptive rock unit names for igneous rocks are based on normalized major element analyses plotted on the total alkalis (Na_2O + K_2O) versus silica (SiO_2) diagram (TAS) of Le Bas and others (1986), Le Bas and Streckeisen (1991), and Le Maitre and others (1989, 2004). New and compiled XRF-geochemical analyses are included in the geodatabase, in a separate shapefile named DRS2018_Geochemistry.shp, and in a Microsoft Excel® spreadsheet named DRS2018_Geochemistry.xlsx. **Table 12-3** explaining fields listed in the spreadsheet can be found below. The locations of all geochemical samples are given in five coordinate systems: UTM Zone 11 (datum = NAD 27, NAD 83, units = meters), Geographic (datum = NAD 27, NAD 83, units = decimal degrees), and Oregon Lambert (datum = NAD 83, HARN, units = international feet).

Samples denoted by lab abbreviation WSU were analyzed by XRF at the Washington State University GeoAnalytical Lab, Pullman, Washington. Analytical procedures for the Washington State University GeoAnalytical Lab are described by Johnson and others (1999) and can be obtained online at https://s3.wp.wsu.edu/uploads/sites/2191/2017/06/Johnson-Hooper-and-Conrey.pdf. Notes for spreadsheet: nd, no data; ¥ original field sample locations in UTM Zone 11 (datum = NAD 83) coordinates.

Table 12-3. Geochemistry spreadsheet field names and descriptions.

Field	Description
SAMPLE_NO	A unique number identifying the sample. E.g., 18 DRSCN 17.
WELL_ID	Well log number for wells. Wells in Harney County preceded by acronym HARN. E.g., HARN 152.
MAP_NO	A unique number identifying the sample on the map plates.
QUADRANGLE	The USGS 7.5′ quadrangle in which the sample is located. E.g., Devine Ridge South.
ELEV_FT	Elevation of sample location in feet. E.g., 1928.
UTMN_NAD27	Meters north in NAD 27 UTM projection, zone 11.
UTME_NAD27	Meters east in NAD 27 UTM projection, zone 11.
LAT_NAD27	Latitude in NAD 27 geographic coordinates.
LONG_NAD27	Longitude in NAD 27 geographic coordinates.
UTMN_NAD83	Meters north in NAD 83 UTM projection, zone 11.
UTME_NAD83	Meters east in NAD 83 UTM projection, zone 11.
LAT_NAD83	Latitude in NAD 83 geographic coordinates.
LONG_NAD83	Longitude in NAD 83 geographic coordinates.
N_83HARN	Feet north in Oregon Lambert NAD 83, HARN, international feet.
E_83HARN	Feet east in Oregon Lambert NAD 83, HARN, international feet.
TERRANE_GR	Geologic group that the sample is assigned to. See GeologicMap, MapUnitPolys in the geodatabase. E.g., Columbia River Basalt Group. See pamphlet and DescriptionOfMapUnits table in the geodatabase.
FORMATION	Geologic formation that the sample is assigned to. See GeologicMap, MapUnitPolys in the geodatabase. E.g., Dalles Formation. See pamphlet and DescriptionOfMapUnits table in the geodatabase.
MEMBER	Geologic member that the sample is assigned to. See GeologicMap, MapUnitPolys in the geodatabase. E.g., Frenchman Springs. See pamphlet and DescriptionOfMapUnits table in the geodatabase.
MAP_UNIT_N	Geologic unit that the sample is assigned to. See GeologicMap, MapUnitPolys in the geodatabase. E.g., Basalt of Gingko. See pamphlet and DescriptionOfMapUnits table in the geodatabase.
MAP_UNIT_L	Unique label identifying the geologic unit that the sample is assigned to. See GeologicMap, MapUnitPolys in the geodatabase. E.g., Tmtr. See pamphlet and DescriptionOfMapUnits table in the geodatabase.

VOLCANIC_FIELD	Volcanic field that the unit is assigned to. In igneous provinces, a well-defined area covered with volcanic rocks with a common geologic history.
TAS_LITHOLOGY	Rock name assigned based on the total alkalis (Na_2O + K_2O) versus silica (SiO_2) diagram (TAS) of Le Bas and others (1986), Le Bas and Streckeisen (1991), and Le Maitre and others (1989). E.g., Basalt, Rhyolite.
[MAJOR ELEMENTS]	SiO_2, Al_2O_3, TiO_2, FeO*, MnO, CaO, MgO, K_2O, Na_2O, P_2O_5. In wt.%.
[TRACE ELEMENTS]	Ni, Cr, Sc, V, Ba, Rb, Sr, Zr, Y, Nb, Ga, Cu, Zn, Pb, La, Ce, Th, Nd, U, Cs, Co, Hf, Sm, Eu, Yb, Lu. In ppm.
LOI	Value for loss on ignition as reported by lab.
FE_2O_3	Iron (III) oxide or ferric oxide reported in original analysis.
FeO	Iron (II) oxide or ferrous oxide reported in original analysis.
REFERENCE	Publication reference, keyed to the reference list in this report.
METHOD	Analytical method used by laboratory that analyzed the sample. E.g., XRF.
LABORATORY	Analytical laboratory that analyzed the sample. E.g., F & M.
NOTES	Special information (e.g., alteration) about certain samples.

Bedding (strike and dip)

Strike and dip measurements of inclined bedding were taken in the map area during this study by traditional compass and clinometer methods. Additional measurements have been compiled from previous workers. Strikes and dips are reported in both quadrant format (e.g., N30W, 15NE) and azimuthal format using the right-hand rule (e.g., 330, 15NE, American convention). Field measured bedding is coded by its appropriate Federal Geographic Data Committee (FGDC) reference number for geologic map symbolization. The measured point data are included in the geodatabase, a separate shapefile named DRS2018_Bedding.shp, and are also provided as a Microsoft Excel spreadsheet named DRS2018_Bedding.xlsx. **Table 12-4** explaining fields listed in the spreadsheet can be found below. The locations of these point data are given in five coordinate systems: UTM Zone 11 (datum = NAD 27, NAD 83, units = meters), Geographic (datum = NAD 27, NAD 83, units = decimal degrees), and Oregon Lambert (datum = NAD 83, HARN, units = international feet). Strike and dip symbols can be properly drawn by the Esri ArcMap product by opening the layer properties, categorizing by type, choosing the appropriate symbol, and rotating the symbol based on the "Strike_Azi" field. (The advanced button allows you to select the rotation field). The rotation style should be set to geographic to maintain the right-hand rule property. Azimuths are given in true north; an additional clockwise correction of about 1.6 degrees is needed to plot strikes and dips properly on the Oregon Lambert conformal conic projection in this area. Notes for spreadsheet: nd, no data.

DOGAMI has developed a routine and model in Esri ArcGIS Model Builder™ to calculate 3-point solutions for SFM-derived bedding. The modeling process incorporates the use of (1) a 5-m SRM-derived DEM (Digital Elevation Model); (2) the registration of three non-collinear points picked along the trace of a geological plane or contact discernable from a 5-m SFM DEM; (3) updating these points with their SFM-derived elevation values; and (4) creating a TIN (triangular irregular network) facet of the three points. The aspect of the TIN facet is equivalent to the dip direction and the slope corresponds to the dip (0˚ to 90˚ degrees). The strike is then determined from the dip direction, subtracting or adding 90˚ based on the right-hand rule (described in paragraph 1 above).

The factors influencing the certainty of SFM-derived bedding are the subjectivity of the digitizer and the clarity of the feature presumed to be indicative of bedding. Where possible aerial photography, combined with a contextual knowledge of the geology of the area, was used to verify bedding features interpreted from the SFM. Agreement of the calculated strikes and dips over small areas, taken together with field measurements and data compiled from previous workers, was used as an accuracy gauge.

Table 12-4. Bedding (strike and dip) spreadsheet field names and descriptions.

Field	Description
STRUCTURE	Type of geologic structure from which feature was determined. E.g., Inclined bedding.
FGDC_REF	An attribute code assigned to each feature, derived from the Federal Geographic Data Committee (FGDC) digital standard for geologic map symbolization. E.g., 6.2.
QUADRANGLE	The USGS 7.5' quadrangle in which the sample is located. E.g., Devine Ridge South.
ELEV_FT	Elevation of data location in feet. E.g., 22.
UTMN_NAD27	Meters north in NAD 27 UTM projection, zone 11.
UTME_NAD27	Meters east in NAD 27 UTM projection, zone 11.
LAT_NAD27	Latitude in NAD 27 geographic coordinates.
LONG_NAD27	Longitude in NAD 27 geographic coordinates.
UTMN_NAD83	Meters north in NAD 83 UTM projection, zone 11.
UTME_NAD83	Meters east in NAD 83 UTM projection, zone 11.
LAT_NAD83	Latitude in NAD 83 geographic coordinates.
LONG_NAD83	Longitude in NAD 83 geographic coordinates.
N_83HARN	Feet north in Oregon Lambert NAD 83, HARN, international feet.
E_83HARN	Feet east in Oregon Lambert NAD 83, HARN, international feet.
TERRANE_GR	Geologic group that the sample is assigned to. See GeologicMap, MapUnitPolys in the geodatabase. E.g., Columbia River Basalt Group.
FORMATION	Geologic formation that the sample is assigned to. See GeologicMap, MapUnitPolys in the geodatabase. E.g., Rattlesnake Tuff Formation.
MEMBER	Geologic member that the sample is assigned to. See GeologicMap, MapUnitPolys in the geodatabase.
MAP_UNIT_N	Geologic unit that the sample is assigned to. See GeologicMap, MapUnitPolys in the geodatabase. E.g., dacite.
MAP_UNIT_L	Unique label identifying the geologic unit that the sample is assigned to. See GeologicMap, MapUnitPolys in the geodatabase. E.g., Toda.
VOLCANIC_FIELD	Volcanic field that the unit is assigned to. In igneous provinces, a well-defined area covered with volcanic rocks with a common geologic history.
STRIKE_QUAD	Strike direction of the inclined plane, stated in a north-directed quadrant format. E.g., N35E.
DIP	Amount of dip, degrees from horizontal, with direction. E.g., 45SE.
STRIKE_AZI	Strike direction of the inclined plane, as determined by employing the right-hand rule (American convention). E.g., 035.
DIP_AZIMUTH	Azimuthal direction of dip. E.g., 125.
DIP_AMOUNT	Amount of dip, degrees from horizontal. E.g., 45.
REFERENCE	Publication reference, keyed to the reference list in this report.
NOTES	Special information (e.g., lidar derived)

Water well logs

The well log spreadsheet is derived from written drillers' logs provided by Oregon Department of Water Resources (OWRD). Well logs vary greatly in completeness and accuracy, so the utility of subsurface interpretations based upon these data can be limited. Water well logs compiled and used for interpretation during this study were not field located. The approximate locations were estimated using tax lot maps, street addresses (coordinates obtained from Google Earth™), and aerial photographs to plot locations on the map. The accuracy of the locations ranges widely, from errors of one-half mile possible for wells located only by section and plotted at the section centroid to a few tens of feet for wells located by address or tax lot number on a city lot with bearing and distance from a corner. At each mapped location the number of the well log is indicated. This number can be combined with the first four letters of the county name (e.g., HARN 5473), to retrieve an image of the well log from the OWRD web site.

Point data are included in the geodatabase, in a separate shapefile named DRS2018_WaterWells.shp, and in a Microsoft Excel spreadsheet named DRS2018_WaterWells.xlsx. **Table 12-5** explaining fields listed in the spreadsheet can be found below. The locations of water well point data are given in six coordinate systems: UTM Zone 11 (datum = WGS 84, NAD 27, NAD 83, units = meters), Geographic (datum

= NAD 27, NAD 83, units = decimal degrees), and Oregon Lambert (datum = NAD 83, HARN, units = international feet).

Lithologies in well intervals listed in the well log spreadsheet can alternate between consolidated and unconsolidated and may be listed as alternating between bedrock and surficial geologic units. This may occur where bedrock units are soft, where paleosols or weak zones lie within bedrock, or where cemented or partly cemented zones alternate with unconsolidated zones in surficial deposits.

Lithologic abbreviations used (alphabetical by group)

UNCONSOLIDATED SURFICIAL UNITS	
Abbreviation	**Description**
a	Ash
bd	Boulders
c	Clay
ch	Clay, hard (often logged as claystone but probably not bedrock)
g	Gravel
gc	Cemented gravel
gs	Gravel and sand (also sandy gravel)
m	Mud
s	Sand
sg	Sand and gravel (also gravelly sand)
st	Silt
ROCK, sedimentary	
ar	Argillite
bc	Breccia
cg	Conglomerate
cs	Claystone
pbs	Pebbly sandstone
sh	Shale
sts	Siltstone
ss	Sandstone
ROCK, igneous	
an	Andesite
b	Basalt
ba	Basaltic andesite
cd	Cinders
pu	Pumice
d	Diorite
gb	Gabbro
gr	Granite
l	Lava
r	Rhyolite
sc	Scoria
t	Tuff
v	Volcanic, undivided
vb	Volcanic breccia
Other	
af	Artificial fill
cl	Coal (lignite)
dg	Decomposed granite
o	Other (drillers unit listed in notes column of spreadsheet)
rk	Rock
sl	Soil
u	Unknown (typically used where a well has been deepened)

Table 12-5. Water well log spreadsheet field names and descriptions.

Field	*Description and Example
TRS	Two digits for township, two digits for range, and two for section; negative if township is south of Willamette baseline. Exception for township and range if they contain a decimal. E.g., −2132.503.
COUNTY	Harney County. E.g., HARN.
GRID	Well log number for wells. Wells in Harney County preceded by acronym HARN (e.g., HARN 53799). E.g., 53779.
WELL_EL_FT	Wellhead elevation in feet as given by Google Earth™ at corresponding WGS 84 location. E.g., 1978.
LOCATED_BY	Google Earth™ elevation for cursor location at a given address. E.g., Google. Google Earth™ elevation at house in vicinity of given address. E.g., House. Pad identifying approximate well location, visible in air photo. E.g., Pad. Approximate taxlot centroid or other best guess for well location using a combination of taxlot maps and aerial photographs. E.g., Taxlot. Owner name. E.g., Owner. Wells located by Oregon Water Resources Department (OWRD) using handheld GPS. E.g., OWRD. GPS coordinates of wellhead included with well log. E.g., GPS. Approximate quarter-quarter-section centroid. E.g., qq. Approximate quarter-section centroid. E.g., q. Approximate fit to sketch map included with well log. E.g., map
LITHOLOGY	Best interpretation of driller’s log using abbreviations above. E.g., g.
BASE_FT	Record base of driller’s interval or, if lithology abbreviation would not change, similar intervals, in feet below wellhead. E.g., 17.
TOP_FT	Calculated top of driller’s interval or similar intervals, in feet below wellhead. E.g., 14.
TOP_EL_FT	Calculated elevation at top of driller’s interval, or similar intervals, in feet above sea level. E.g., 86.
BASE_EL_FT	Calculated elevation at base of driller’s interval, or similar intervals, in feet above sea level. E.g., 83.
BEDRK_LITH	Lists bedrock lithologies, when encountered, abbreviations listed above. E.g., b.
BEDRK_ELEV	Calculated elevation at which bedrock or soil over bedrock was first encountered, in feet above sea level. E.g., 1924.
TAX_LOT	Taxlot number. Where it is determined that a taxlot number is used more than once in the section then the appropriate subdivision of the section is indicated in the notes field. E.g., 800.
COLOR	Color of interval as reported by the well driller. E.g., green.
NOTES	Notes about the stratigraphic interval as originally described by the well driller.
MAP_LABEL	Geologic unit interpreted in subsurface based on drillers log and designated by map unit label used in accompanying geodatabase. Intervals labeled “suna” (surface unit not applicable) are those where the lithology as interpreted by the original drillers’ log do not correspond; also denotes intervals in the subsurface where a precise unit label cannot be applied. E.g., Tb.
QUADRANGLE	The USGS 7.5′ quadrangle in which the sample is located. E.g., Devine Ridge South.
UTMN_WGS84	Meters north in WGS84 UTM projection, zone 11.
UTME_WGS84	Meters east in WGS84 UTM projection, zone 11.
UTMN_NAD27	Meters north in NAD 27 UTM projection, zone 11.
UTME_NAD27	Meters east in NAD 27 UTM projection, zone 11.
LAT_NAD27	Latitude in NAD 27 geographic coordinates.
LONG_NAD27	Longitude in NAD 27 geographic coordinates.
UTMN_NAD83	Meters north in NAD 83 UTM projection, zone 11.
UTME_NAD83	Meters east in NAD 83 UTM projection, zone 11.
LAT_NAD83	Latitude in NAD 83 geographic coordinates.
LONG_NAD83	Longitude in NAD 83 geographic coordinates.
N_83HARN	Feet north in Oregon Lambert NAD 83, HARN, international feet.
E_83HARN	Feet east in Oregon Lambert NAD 83, HARN, international feet.

*Well location given in six coordinate systems calculated by reprojecting original WGS 84 UTM, zone 11 locations.